SoxC Transcription Factors Promote Contralateral Retinal Ganglion Cell Differentiation and Axon Guidance in the Mouse Visual System

Highlights

- SoxC transcription factors are highly expressed in contralateral RGCs

- SoxC factors promote contralateral RGC differentiation via Notch signaling

- SoxC factors regulate contralateral RGC axon outgrowth on chiasm cells

- SoxC factors influence Nr-CAM and Plexin-A1 expression

Authors

Takaaki Kuwajima, Célia A. Soares, Austen A. Sitko, Véronique Lefebvre, Carol Mason

Correspondence

tk2288@columbia.edu (T.K.), cam4@columbia.edu (C.M.)

In Brief

Kuwajima et al. identify SoxC transcription factors in the differentiation and guidance of retinal ganglion cells that project contralaterally. The SoxC factors regulate Hes5 in the Notch pathway and expression of guidance receptors Plexin-A1 and Nr-CAM, respectively.

Neuron

Article

CellPress

SoxC Transcription Factors Promote Contralateral Retinal Ganglion Cell Differentiation and Axon Guidance in the Mouse Visual System

Takaaki Kuwajima,[1,*] Célia A. Soares,[1] Austen A. Sitko,[2] Véronique Lefebvre,[4] and Carol Mason[1,2,3,5,*]
[1]Department of Pathology and Cell Biology
[2]Department of Neuroscience
[3]Department of Ophthalmology
College of Physicians and Surgeons, Columbia University, New York, NY 10032, USA
[4]Department of Cellular and Molecular Medicine, Orthopaedic and Rheumatologic Research Center, Cleveland Clinic Lerner Research Institute, Cleveland, OH 44195, USA
[5]Lead Contact
*Correspondence: tk2288@columbia.edu (T.K.), cam4@columbia.edu (C.M.)
http://dx.doi.org/10.1016/j.neuron.2017.01.029

SUMMARY

Transcription factors control cell identity by regulating diverse developmental steps such as differentiation and axon guidance. The mammalian binocular visual circuit is comprised of projections of retinal ganglion cells (RGCs) to ipsilateral and contralateral targets in the brain. A transcriptional code for ipsilateral RGC identity has been identified, but less is known about the transcriptional regulation of contralateral RGC development. Here we demonstrate that SoxC genes (*Sox4, 11*, and *12*) act on the progenitor-to-postmitotic transition to implement contralateral, but not ipsilateral, RGC differentiation, by binding to Hes5 and thus repressing Notch signaling. When SoxC genes are deleted in postmitotic RGCs, contralateral RGC axons grow poorly on chiasm cells in vitro and project ipsilaterally at the chiasm midline in vivo, and Plexin-A1 and Nr-CAM expression in RGCs is downregulated. These data implicate SoxC transcription factors in the regulation of contralateral RGC differentiation and axon guidance.

INTRODUCTION

During the development of neural circuits, axons are guided to their targets in the brain by molecular cues along their paths. The expression of axonal receptors that respond to such guidance cues at distinct points along pathways is regulated by transcriptional mechanisms (Butler and Tear, 2007; Jessell, 2000; Polleux et al., 2007). As such, specific transcription factors (TFs) establish cell subtype identity through shaping molecular programs for axon guidance.

Retinal ganglion cell (RGC) axon pathway choice at the optic chiasm midline to project ipsilaterally or contralaterally is key to establishing the binocular visual circuit in mammals. Ipsilateral RGCs arise from the ventrotemporal (VT) retina and contralateral RGCs from retinal regions outside of the VT sector (non-VT) from embryonic day 14 (E14) to E17 and from the VT retina from E17.5 to postnatal day 0 (P0) (Erskine and Herrera, 2014; Petros et al., 2008).

The molecular pathways underlying the ipsilateral retinal projection are known for the mouse visual system. The guidance receptor EphB1 is upregulated in VT RGCs that project ipsilaterally from E14 to E17 and interacts with its ligand ephrin-B2 on radial glial cells at the optic chiasm, leading to the formation of the ipsilateral projection (Petros et al., 2009; Williams et al., 2003). The zinc finger TF Zic2 governs ipsilateral RGC identity and drives expression of EphB1 and the serotonin transporter (Sert), which functions in ipsilateral RGCs in activity-dependent refinement in thalamic and midbrain targets (García-Frigola et al., 2008; García-Frigola and Herrera, 2010; Herrera et al., 2003; Lee et al., 2008).

Guidance receptors mediating the contralateral retinal projection have been identified. Plexin-A1 and Nr-CAM expressed in Zic2-negative RGCs promote contralateral axon outgrowth through interactions with the guidance cues, semaphorin6D and Nr-CAM, which are expressed on midline radial glia, and with Plexin-A1 on early-born neurons at the caudal optic chiasm (Kuwajima et al., 2012; Williams et al., 2006). In addition, the semaphorin receptor Neuropilin1 is expressed in these same RGCs and participates in attracting contralateral axons to the midline by binding to its ligand VEGF at the optic chiasm (Erskine et al., 2011).

To date, only one TF, the LIM homeodomain protein Islet2, is known to direct contralateral RGC axon guidance (Pak et al., 2004). However, Islet2 is expressed in only ∼30% of RGCs in non-VT retina and primarily regulates the late-born contralateral RGC projection that extends from VT retina at E18. The expression pattern and function of Islet2 in RGC axon guidance do not match those of the contralateral RGC guidance receptors identified to date. Therefore, other TFs must exist that direct midline crossing through controlling expression of contralateral RGC-specific guidance receptors.

The 5′ non-coding regions of *Plexna1* (encoding Plexin-A1) and *Nrcam* (encoding neural cell adhesion molecule, Nr-CAM) contain their regulatory sequences (Sánchez-Arrones et al.,

CellPress

2013; Wong et al., 2003). Through an in silico search, we found that these non-coding regions are conserved across binocular species. We identified the Sox family of TFs, which shares a highly conserved *Sry*-related high-mobility-group DNA-binding domain, as having binding sites to *Plexna1* and *Nrcam*. Within this family, the SoxC genes (Sox4, Sox11, and Sox12) are expressed in developing RGCs (Hoser et al., 2008; Jiang et al., 2013; Usui et al., 2013). Moreover, expression of Plexin-A1 is downregulated in *Sox4*-depleted cancer cells (Huang et al., 2012). Sox4 and Sox11 regulate corticospinal neuron trajectory by activating *Fezf2* expression via binding to enhancer elements conserved among vertebrates (Shim et al., 2012). Therefore, we considered the SoxC TFs as good candidates for regulating expression of *Plxna1* and *Nrcam* and thus the contralateral RGC axon trajectory at the optic chiasm midline.

Sox4 and Sox11 function in retinal morphogenesis and RGC neurogenesis beginning at E11, and *Sox4/Sox11* conditional mutant mice display severe hypoplasia of the developing retina, leading to reduced size of the retina and thinner RGC and inner plexiform layers in the adult (Jiang et al., 2013; Usui et al., 2013). However, whether SoxC TFs are expressed in all or a subset of RGCs (e.g., ipsi- versus contralaterally-projecting), whether they direct differentiation of these RGCs, and whether SoxC TFs play a role in axon guidance at the optic chiasm midline were not known.

Here we examine the expression and role of SoxC (Sox4, 11, and 12) TFs in RGC differentiation and axon guidance at the chiasm midline. We show that SoxC genes are highly expressed in RGCs in regions of the retina where contralateral RGCs reside, from E13.5 onward. Further, we identify a novel transcriptional pathway involving the SoxC TFs in regulating contralateral RGC differentiation and guidance post-differentiation.

RESULTS

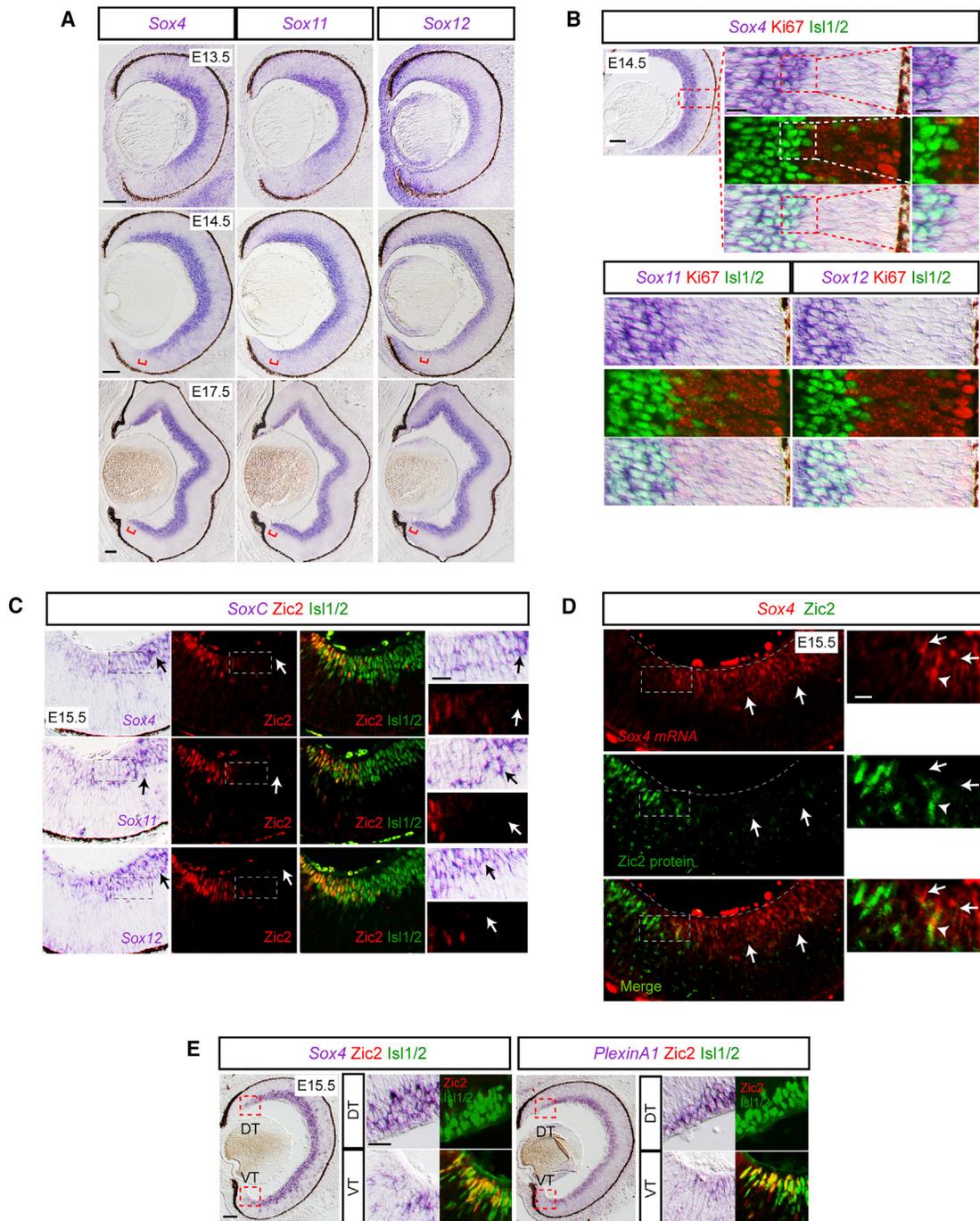### SoxC Genes Are Expressed in Contralateral but Not Ipsilateral RGCs

To relate SoxC expression to the spatial and temporal aspects of the formation of the ipsi- and contralateral RGC projections, we examined expression patterns of SoxC genes (*Sox4*, *Sox11*, and *Sox12*) in the retina at the three phases of RGC axon extension during optic chiasm formation: E12–13.5, when the first RGCs extend from central retina both contralaterally and transiently, ipsilaterally (Soares and Mason, 2015); E14–E17, when the permanent ipsilaterally projecting RGCs extend from the VT retina and contralaterally projecting RGCs from non-VT retina; and E17.5–P0, when contralaterally projecting RGCs extend from VT as well as non-VT retina (Figure 1A) (Petros et al., 2008). *Sox4*, *Sox11*, and *Sox12* mRNAs are highly expressed in the central retina at E13.5 and by E14.5 in RGCs in more peripheral regions of the retina, excluding VT retina (Figure 1A). After E17.5, SoxC mRNA expression extends into VT retina, where late-born contralateral RGCs are situated (Figure 1A). Ki67 and Islet1/2 are markers for progenitors and mature RGCs, respectively (Bhansali et al., 2014; Pan et al., 2008; Usui et al., 2013). At E14.5, SoxC genes are expressed in differentiated, Islet1/2$^+$ RGCs but are absent from Ki67$^+$ progenitors (Figure 1B).

From E14 onward, the transcription factor Zic2 is expressed in VT RGCs that project ipsilaterally (Herrera et al., 2003). In situ hybridization for SoxC TFs and immunohistochemistry for Zic2 were performed on the same sections (Figures 1C, 1D, and S1A). At E15.5 and E18.5, the majority of SoxC TF-positive RGCs lack Zic2. However, at the border of the VT region where Zic2 is highly expressed and adjacent to the SoxC TF-expressing zone, a few RGCs weakly express both Zic2 and *Sox4*: in a 200 μm × 200 μm region of VT retina, 4.3% (1.8/42.6 cells) and 7.9% (5/63.1 cells) of Sox4-positive cells express Zic2 at E15.5 and E18.5, respectively; n = 3 embryos at each age (Figures 1D and S1A). Moreover, at E15.5, SoxC TFs are expressed by RGCs expressing the contralateral RGC receptor *Plexin-A1* in non-VT (e.g., dorsotemporal [DT]) retina, where contralateral RGCs arise, but not in VT retina where Plexin-A1 is absent at this stage (Figure 1E). These data establish that SoxC genes are expressed predominantly in RGCs that project contralaterally, suggesting that SoxC TFs may have a selective role in contralateral RGC development.

SoxC TFs Regulate Contralateral but Not Ipsilateral RGC Differentiation

We next investigated how *Sox4*, *Sox11*, and *Sox12* function in RGC development by deletion of these genes in *Sox4*$^{flox/flox}$ *Sox11*$^{flox/flox}$*Sox12*$^{-/-}$ (*Sox4*$^{f/f}$*Sox11*$^{f/f}$*Sox12*$^{-/-}$) triple conditional mutant embryos at E14.5, when ipsilateral and contralateral RGCs are spatially segregated into VT and non-VT retina, respectively. We electroporated *Cre* recombinase plasmid into the *Sox4*$^{f/f}$*Sox11*$^{f/f}$*Sox12*$^{-/-}$ contralateral retina ex vivo to delete *Sox4* and *Sox11*, with constitutive deletion of *Sox12*, as *Sox12*$^{-/-}$ single mutant mice are viable after birth and develop normally (Bhattaram et al., 2010) (Figure 2).

We next examined whether SoxC TFs differentially affect maturation of contralateral (DT) and ipsilateral (VT) retinal cells (Figures 2A–2D). *CAG-GFP* and *CAG-Cre* plasmids were electroporated ex vivo into E14.5 WT or *Sox4*$^{f/f}$*Sox11*$^{f/f}$*Sox12*$^{-/-}$ DT retina to generate WT or *Sox4*$^{-/-}$*Sox11*$^{-/-}$*Sox12*$^{-/-}$ GFP$^+$ cells, respectively, and *CAG-GFP* alone into *Sox4*$^{f/f}$*Sox11*$^{f/f}$ *Sox12*$^{-/-}$ retina to generate *Sox12*$^{-/-}$ GFP$^+$ cells. After culturing the entire retina for 24 hr, retinae were dissociated into a single-cell suspension, plated, and kept in vitro for 48 hr to allow electroporated GFP$^+$ retinal precursors to differentiate into RGCs (Figures S2A–S2D). 95.6% ± 0.7% of GFP$^+$ cells express Cre (>300 of total GFP$^+$ cells counted, n = 3 cultures). Cultures of *Sox4*$^{-/-}$*Sox11*$^{-/-}$*Sox12*$^{-/-}$ DT retinal cells contained fewer Islet1/2$^+$/GFP$^+$ cells and more Ki67$^+$/GFP$^+$ cells compared with WT or *Sox12*$^{-/-}$ DT retinal cell cultures (Figures 2A–2D). Brn3a is a marker for RGCs, especially contralateral RGCs (Quina et al., 2005). Fewer *Sox4*$^{-/-}$*Sox11*$^{-/-}$*Sox12*$^{-/-}$ DT retinal cells expressed Brn3a compared with WT cells (Brn3a$^+$/GFP$^+$ cells in WT = 60.2% ± 4.2 versus *Sox4*$^{-/-}$*Sox11*$^{-/-}$*Sox12*$^{-/-}$ = 8.1% ± 2.5, >300 of total GFP$^+$ cells counted for each condition; n = 3 cultures; p < 0.001, Student's t test) (data not shown). In contrast, *Sox4*$^{-/-}$*Sox11*$^{-/-}$*Sox12*$^{-/-}$ VT GFP$^+$ retinal cells displayed little alteration of the number of differentiated RGCs versus progenitor cells, similar to WT or *Sox12*$^{-/-}$ VT retinal cells (Figures 2A–2D). These data thus suggest that SoxC TFs are required for contralateral but not ipsilateral RGC differentiation.

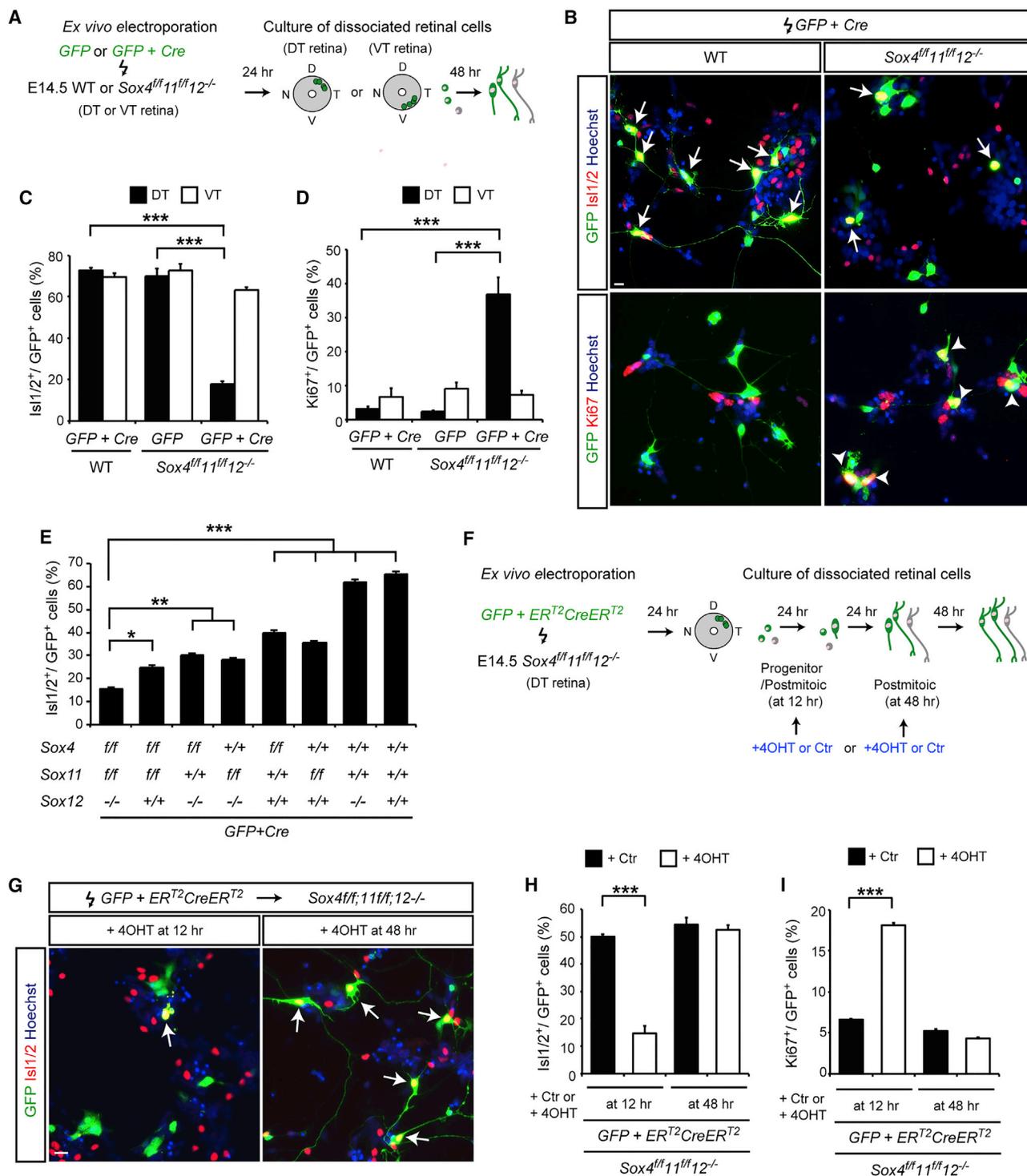**Figure 1. SoxC Genes Are Expressed in Regions of the Retina Giving Rise to Contralateral RGCs**

(A) Expression of *Sox4*, *Sox11*, and *Sox12* mRNAs in the RGC layer at E13.5, E14.5, and E17.5. Red bracket points to VT retina.

(B) Expression of *Sox4*, *Sox11*, and *Sox12* mRNAs in RGCs (Islet1/2$^+$), not but in progenitor cells (Ki67$^+$) at E14.5.

(C and D) *Sox4*, *Sox11*, and *Sox12* mRNAs are for the most part not co-expressed with Zic2 protein in VT RGCs at E15.5 (arrows), but a few RGCs weakly express both Zic2 and SoxC (arrowheads) in the same section.

(E) Similar expression patterns of *Sox4* and *Plexin-A1* mRNAs in DT, but not Zic2$^+$ VT, RGCs at E15.5.

See also Figure S1. DT, dorsotemporal; VT, ventrotemporal. Scale bars, 100 μm in (A), (B), and (E) (whole retina); 20 μm in (B)–(E) (high magnification of retinal cells).

CellPress

Figure 2. SoxC TFs Regulate Contralateral but Not Ipsilateral RGC Differentiation

(A) Schema of ex vivo electroporation of *CAG-GFP* and *CAG-Cre* plasmids into E14.5 WT or *Sox4^{f/f}Sox11^{f/f}Sox12^{-/-}* contralateral (DT) or ipsilateral (VT) retina and cell cultures.

(B) Representative images of Islet1/2$^+$/GFP$^+$ RGCs (arrows) and Ki67$^+$/GFP$^+$ progenitor cells (arrowheads) in WT and *Sox4^{-/-}Sox11^{-/-}Sox12^{-/-}* DT cultures.

(C and D) Quantification of Islet1/2$^+$/GFP$^+$ cells (%) (C) and Ki67$^+$/GFP$^+$ cells (%) (D) in WT, *Sox12^{-/-}*, and *Sox4^{-/-}Sox11^{-/-}Sox12^{-/-}* DT or VT dissociated cultures (>380 of total GFP$^+$ cells counted for each condition; n = 4–5; two-way ANOVA).

(E) Magnitude of RGC differentiation defects in *Sox4^{-/-}Sox11^{-/-}Sox12^{-/-}* DT retinal cells compared to WT, SoxC single or double mutant DT retinal cells (>275 of total GFP$^+$ cells counted for each condition; n = 3; one-way ANOVA).

(legend continued on next page)

CellPress

Since $Sox12^{-/-}$ DT retina differentiate into postmitotic RGCs as in WT retina (Figures 2C and 2D), we investigated the overlapping function of SoxC TFs in RGC differentiation (Figure 2E). $Sox4^{-/-}Sox11^{-/-}Sox12^{-/-}$ triple mutant DT cultures had the fewest Islet1/2$^+$/GFP$^+$ cells compared with WT, $Sox4^{-/-}$ or $Sox11^{-/-}$ single, or $Sox4^{-/-}Sox11^{-/-}$, $Sox4^{-/-}Sox12^{-/-}$, or $Sox11^{-/-}Sox12^{-/-}$ double mutants. Thus, SoxC TFs similarly regulate the differentiation of contralateral RGCs.

We next asked whether SoxC TFs regulate RGC differentiation as cells transit from progenitor to postmitotic neuron and/or maintain the postmitotic differentiation state, by deleting SoxC genes at different times. To delete SoxC genes with temporal control, we utilized CAG-$ER^{T2}CreER^{T2}$ and administered 4-hydroxytamoxifen (4OHT) to dissociated retinal cell cultures to elicit Cre/$loxP$-mediated recombination, reported to occur within 24 hr in the retina in vivo (Matsuda and Cepko, 2007) and within 12 hr in vitro (data not shown). CAG-GFP and CAG-$ER^{T2}CreER^{T2}$ plasmids were co-electroporated into E14.5 $Sox4^{f/f}Sox11^{f/f}Sox12^{-/-}$ DT retina, and $Sox4^{-/-}Sox11^{-/-}Sox12^{-/-}$ DT GFP$^+$ cells and $Sox12^{-/-}$ GFP$^+$ cells were generated with or without adding 4OHT to the medium, respectively (Figure 2F). 94.8% ± 0.8% of GFP$^+$ cells in dissociated retinal cell culture express Cre in the nucleus after incubation with 4OHT for 24 hr (>300 of total GFP$^+$ cells counted, n = 3 cultures) (data not shown). 4OHT addition to dissociated retinal cell cultures at 12 hr, at the transition point between the progenitor state and differentiation, produced cultures of $Sox4^{-/-}Sox11^{-/-}Sox12^{-/-}$ DT retinal cells (Figure S2). Fewer Islet1/2$^+$/GFP$^+$ cells and more Ki67$^+$/GFP$^+$ cells were observed compared with cultures without 4OHT (Figures 2G–2I). However, when 4OHT was applied to dissociated retinal cells at 48 hr, at the time when most cells are postmitotic (Figure S2), $Sox4^{-/-}Sox11^{-/-}Sox12^{-/-}$ and $Sox12^{-/-}$ DT retinal cell cultures had similar numbers of Islet1/2$^+$ cells and Ki67$^+$ cells (Figures 2G–2I). Apoptotic features such as nuclear fragmentation and DNA condensation were not detected in over 95% of $Sox4^{-/-}Sox11^{-/-}Sox12^{-/-}$ and $Sox12^{-/-}$ DT GFP$^+$ retinal cells ($Sox4^{-/-}Sox11^{-/-}Sox12^{-/-}$ = 4.9 ± 1.0 versus $Sox12^{-/-}$ = 3.6 ± 1.1; n = 4 cultures; N.S., Student's t test) (data not shown). These data suggest that SoxC TFs regulate contralateral RGC differentiation at the transition between progenitor and early postmitotic state but that these TFs do not affect the RGC post-differentiation state or survival.

SoxC TFs Promote Contralateral RGC Differentiation by Antagonizing Notch-Hes5 Signaling

Notch-Hes5 signaling is important for driving proliferation in the chick retina and mouse cerebral cortex (Nelson et al., 2006; Tiberi et al., 2012), and in the hippocampus, the $Hes5$ gene is a direct target of Sox21, which regulates hippocampal adult neurogenesis (Matsuda et al., 2012). Thus, we asked whether

SoxC TFs might regulate contralateral RGC differentiation by antagonizing Notch-Hes5 signaling.

First, we examined expression patterns of $Hes5$ and $Notch1$ genes in the developing retina (Figures 3A and S3). $Hes5$ is expressed in Ki67$^+$ progenitor cells in the neuroblastic layer but not in the ciliary marginal zone (CMZ), which is a source of RGCs (Bélanger et al., 2017; Marcucci et al., 2016; Wang et al., 2016). $Notch1$ is also highly expressed in the neuroblastic layer and moderately expressed in the RGC layer. In contrast, $Sox4$ is expressed in Islet1/2$^+$ postmitotic RGCs. These data indicate that $Hes5$ and SoxC genes have complementary expression in the developing retina.

Second, we investigated whether SoxC TFs modulate Notch-regulated transcriptional activity of the $Hes5$ promoter, which contains binding sites both for Sox TFs and the Notch1 intracellular domain (NICD) (Matsuda et al., 2012). Whereas NICD alone upregulated reporter activity of the $Hes5$ promoter, Sox4, Sox11, and Sox12 antagonized this Notch-driven transcriptional activation (Figure 3B). To investigate functional antagonistic interactions of SoxC TFs with Notch-Hes5 signaling in RGC differentiation, we next tested whether overexpression of Hes5 inhibits contralateral RGC differentiation (Figures 3C–3E). E14.5 WT DT retina was co-electroporated with CAG-GFP and CAG-$Hes5$ plasmids: overexpression of Hes5 led to a decrease in Islet1/2$^+$/GFP$^+$ cells and an increase in Ki67$^+$/GFP$^+$ cells. In contrast, overexpression of Hes5 in $Sox4^{-/-}Sox11^{-/-}Sox12^{-/-}$ mutant DT retina did not change the number of Ki67$^+$/GFP$^+$ cells compared to $Sox4^{-/-}Sox11^{-/-}Sox12^{-/-}$ mutant DT cells. However, after overexpression of Hes5 in VT retina, VT RGC differentiation was unaffected (Figures S4A and S4B). These results suggest that defects in contralateral RGC differentiation are induced by loss-of-function of SoxC genes and gain-of-function of Hes5 in the retina.

DAPT, an inhibitor of the gamma-secretase complex, blocks Notch activity and reduces Hes5 expression levels and promotes RGC differentiation in developing mouse and chick retina (Nelson et al., 2006, 2007). To investigate whether defects in RGC differentiation in SoxC mutants could be rescued by repressing Notch activity with DAPT, $Sox4^{-/-}Sox11^{-/-}Sox12^{-/-}$ GFP$^+$ cells were cultured in the presence of DAPT (Figures 3F–3H). The reduced number of Islet1/2$^+$/GFP$^+$ cells and the increased number of Ki67$^+$/GFP$^+$ cells observed in $Sox4^{-/-}Sox11^{-/-}Sox12^{-/-}$ DT retinal cells were restored to WT levels by DAPT. VT retinal cells from WT and $Sox4^{-/-}Sox11^{-/-}Sox12^{-/-}$ mutant retinae were not affected by DAPT addition (Figures S4C and S4D).
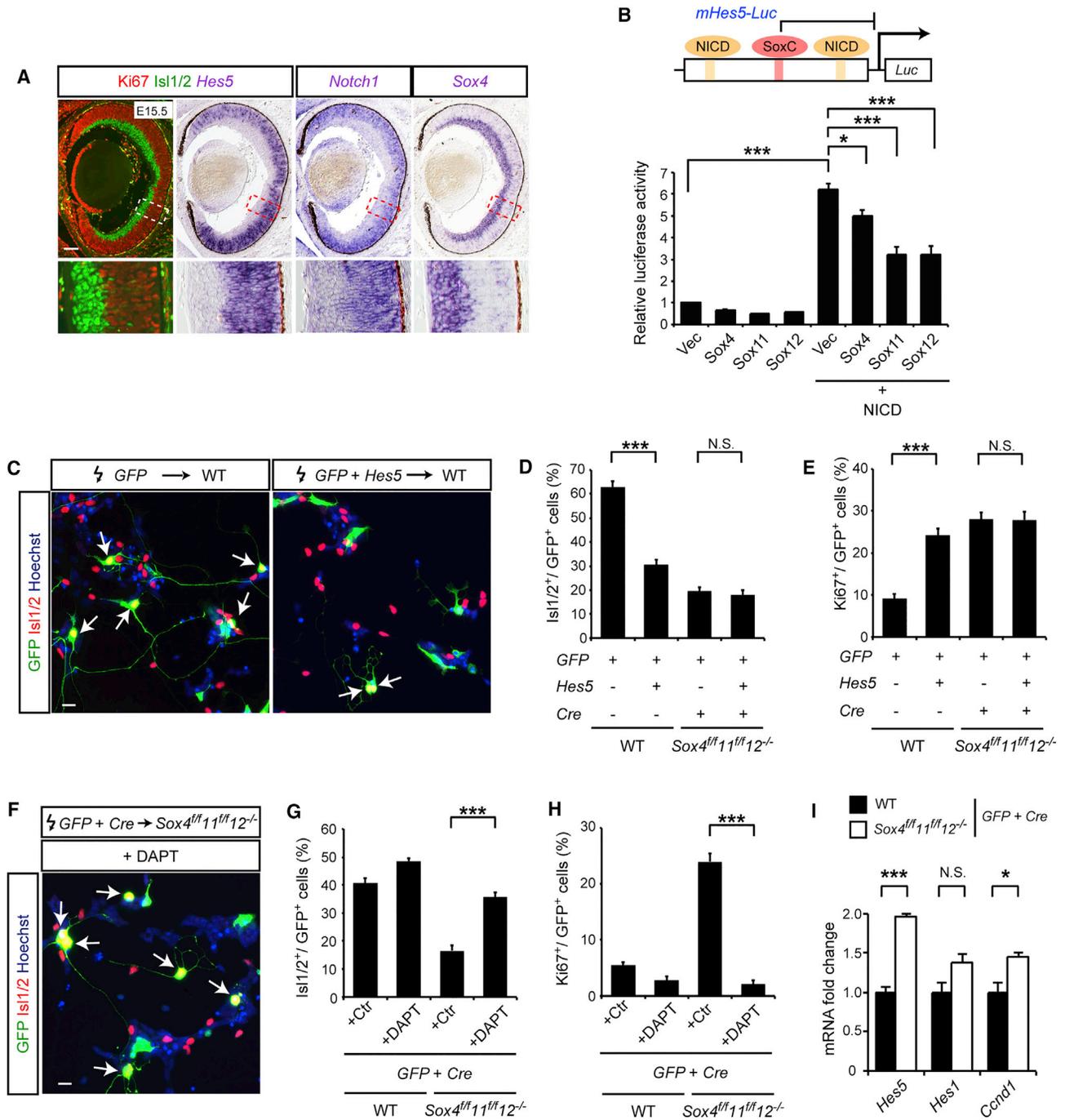
To further examine whether the Notch pathway, especially Hes5, is specifically involved in RGC differentiation defects in $Sox4^{-/-}Sox11^{-/-}Sox12^{-/-}$ retinal cells, we analyzed expression levels of $Hes5$, $Hes1$, and $Ccnd1$ (encoding CyclinD1) mRNAs,

(F) Schema of ex vivo electroporation of both CAG-GFP and CAG-$ER^{T2}CreER^{T2}$ plasmids into E14.5 $Sox4^{f/f}Sox11^{f/f}Sox12^{-/-}$ DT retina to generate $Sox4^{-/-}Sox11^{-/-}Sox12^{-/-}$ or $Sox12^{-/-}$ GFP$^+$ cells during the progenitor/postmitotic state (at 12 hr in dissociated retinal cell cultures) or at the postmitotic state (at 48 hr in dissociated retinal cultures), by adding 4-hydroxytamoxifen (4OHT) or ethanol alone (control, Ctr).

(G) Representative images of Islet1/2$^+$/GFP$^+$ cells after deletion of SoxC genes at 12 or 48 hr in dissociated retinal cultures (arrows).

(H and I) Quantification of Islet1/2$^+$/GFP$^+$ cells (%) (H) and Ki67$^+$/GFP$^+$ cells (%) (I) from DT retina where all SoxC genes were deleted during the progenitor/postmitotic or at postmitotic state (>510 of total GFP$^+$ cells counted for each condition; n = 4; two-way ANOVA).

See also Figure S2. DT, dorsotemporal; VT, ventrotemporal. Scale bars, 10 μm. *p < 0.05, **p < 0.01, ***p < 0.001.

Figure 3. SoxC TFs Repress Notch-Hes5 Signaling to Promote Contralateral RGC Differentiation

(A) Expression of *Hes5* and *Notch1* mRNAs in Ki67$^+$ progenitor cells and *Sox4* mRNA in Islet1/2$^+$ RGCs at E15.5.

(B) Luciferase assay in HEK293 cells transfected with combinations of expression vectors for the Notch intracellular domain (NICD) (1.2 μg) and/or SoxC (4, 11, 12) (2.4 μg) with a reporter vector including the mouse *Hes5* promoter region (0.4 μg) and a *Renilla* luciferase construct (0.03 μg). Data are presented as fold change in relative luciferase activity normalized to the mean of empty vector (Vec). n = 4; two-way ANOVA.

(C) Representative images of Islet1/2$^+$ RGCs after overexpression of *CAG-Hes5* plasmid into WT DT retina (arrows).

(D and E) Quantification of Islet1/2$^+$/GFP$^+$ cells (%) (D) and Ki67$^+$/GFP$^+$ cells (%) (E) in WT or *Sox4$^{-/-}$Sox11$^{-/-}$Sox12$^{-/-}$* DT retina when Hes5 is overexpressed.(>360 of total GFP$^+$ cells counted for each condition; n = 4; one-way ANOVA).

(F) A representative image of Islet1/2$^+$ RGCs in *Sox4$^{-/-}$Sox11$^{-/-}$Sox12$^{-/-}$* DT retinal cells with DAPT added to the medium (+ DAPT) (arrows).

(legend continued on next page)

the latter two genes important for maintaining the retinal progenitor state and preventing RGC differentiation (Das et al., 2009; Nelson et al., 2006; Ohtsuka et al., 1999). After electroporation of *CAG-GFP* and *CAG-Cre* plasmids, cells from the WT or $Sox4^{-/-}Sox11^{-/-}Sox12^{-/-}$ GFP$^+$ region of the DT retina were cultured for 48 hr, and expression levels were measured by qPCR. *Hes5* mRNA is the most upregulated gene (1.96-fold activation) among these three genes in SoxC mutant retinal cells (Figure 3I).

Taken together, these data suggest that Notch-Hes5 signaling maintains the progenitor state in cells in the regions of the retina giving rise to contralaterally projecting RGCs and that reducing activity of Notch-Hes5 signaling can rescue defects in $Sox4^{-/-}Sox11^{-/-}Sox12^{-/-}$ mutant RGC differentiation.

SoxC Mutants Display Defects in Contralateral RGC Differentiation In Vivo

To investigate the function of SoxC TFs in vivo, *CAG-GFP* alone or *CAG-GFP* and *CAG-Cre* plasmids were electroporated into the retina away from VT retina of WT or $Sox4^{f/f}Sox11^{f/f}Sox12^{-/-}$ mice at E14.5, to generate WT, $Sox12^{-/-}$, or $Sox4^{-/-}Sox11^{-/-}Sox12^{-/-}$ GFP$^+$ cells (Figure 4A). 92.4% ± 0.3% of GFP$^+$ cells expressed Cre at E18.5 (>350 of total GFP$^+$ cells counted, n = 3 embryos). We then analyzed the number of Islet1/2$^+$ RGCs or Ki67$^+$ progenitor cells at E18.5 (Figure 4B). In both WT and $Sox12^{-/-}$ retinae, ~50% of GFP$^+$ cells expressed Islet1/2 and ~20% of GFP$^+$ cells expressed Ki67. In contrast, in $Sox4^{-/-}Sox11^{-/-}Sox12^{-/-}$ retinae, only 11% of GFP$^+$ cells expressed Islet1/2 and ~60% of GFP$^+$ cells expressed Ki67, and the latter cells were positioned in the progenitor cell layer (Figures 4B–4D). These data suggest that SoxC TFs can influence contralateral RGC differentiation in vivo.

SoxC Mutant Contralateral RGC Axon Outgrowth Is Impaired on Chiasm Cells

Although SoxC TFs appear to be necessary for contralateral RGC differentiation, it remains unclear whether SoxC TFs might also mediate axon growth and guidance at the chiasm midline. To address this, we employed two experimental strategies to manipulate SoxC expression in RGCs without perturbing RGC differentiation.

Defects in RGC differentiation in SoxC mutant DT retina were attenuated by DAPT, which blocks Notch signaling, as shown above, and only then could long axons be detected (Figures 3F–3H). We therefore analyzed GFP$^+$ axon outgrowth in retinal explant cultures with or without chiasm cells in the presence or absence of DAPT (Figures S5A–S5C). Without chiasm cells, $Sox4^{-/-}Sox11^{-/-}Sox12^{-/-}$ GFP$^+$ DT retinal explants display fewer GFP$^+$ axons than WT or $Sox12^{-/-}$ GFP$^+$ DT explants, while treatment with DAPT led to robust GFP$^+$ axon outgrowth of $Sox4^{-/-}Sox11^{-/-}Sox12^{-/-}$ GFP$^+$ DT explants. However, in the presence of chiasm cells, even with addition of DAPT, axon outgrowth of $Sox4^{-/-}Sox11^{-/-}Sox12^{-/-}$ GFP$^+$ DT explants

was poor (Figures S5B and S5C). In contrast, $Sox4^{-/-}Sox11^{-/-}Sox12^{-/-}$ and WT GFP$^+$ VT retinal explants displayed similar GFP$^+$ axon outgrowth with and without chiasm cells (Figures S6A and S6B). Therefore, this experiment indicates that blocking Notch signaling can rescue differentiation and axon outgrowth in SoxC mutant RGCs when on laminin, but not when they are on chiasm cells (Figures S5B and S5C). These data suggest that SoxC TFs are necessary to regulate axon outgrowth on chiasm cells independent of Notch signaling, potentially via other pathways regulating guidance receptors.

Next, we designed an experiment to conditionally delete SoxC genes and analyze axon outgrowth on chiasm cells without perturbing Notch signaling. Since deletion of SoxC genes in postmitotic RGCs in vitro does not perturb RGC differentiation and neurites can extend (Figures 2F–2I), we electroporated *CAG-GFP* and $CAG-ER^{T2}CreER^{T2}$ plasmids into E14.5 $Sox4^{f/f}Sox11^{f/f}Sox12^{-/-}$ DT retina and then added 4OHT to generate $Sox4^{-/-}Sox11^{-/-}Sox12^{-/-}$ GFP$^+$ DT explants cultured on laminin alone or on chiasm cells after axons had extended (Figures 5B). $Sox4^{-/-}Sox11^{-/-}Sox12^{-/-}$ GFP$^+$ DT retinal explants displayed robust GFP$^+$ axon outgrowth on laminin without chiasm cells, as did WT and $Sox12^{-/-}$ GFP$^+$ DT explants. However, $Sox4^{-/-}Sox11^{-/-}Sox12^{-/-}$ GFP$^+$ DT retinal explants grown on chiasm cells showed a large reduction in axon outgrowth compared with WT and $Sox12^{-/-}$ DT explants (Figures 5C and 5D). These data suggest that even if axons can extend, SoxC TFs are required for contralateral RGC outgrowth on chiasm cells, potentially by regulating guidance receptors on RGCs needed to respond to signals from chiasm cells.
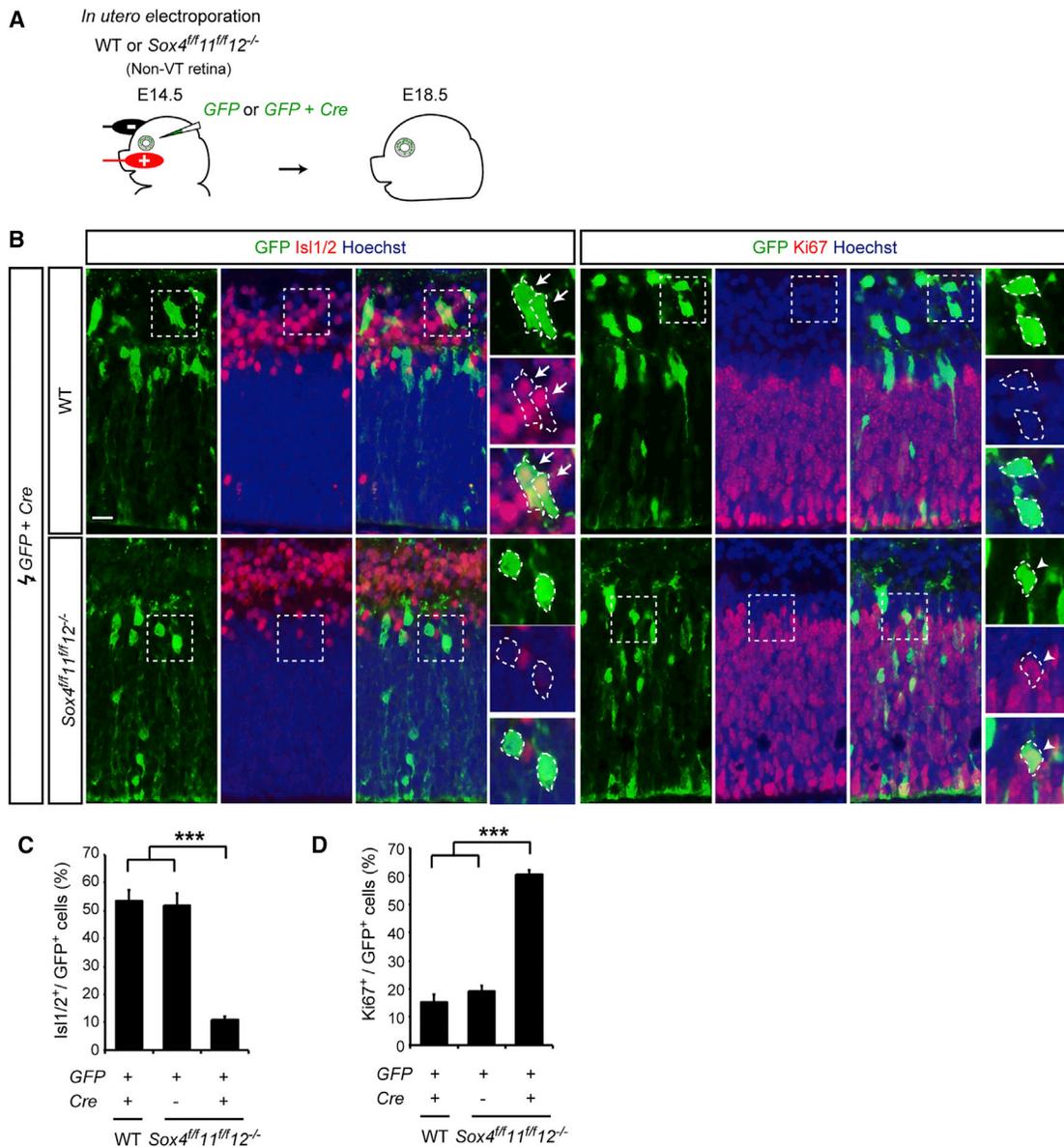
Midline Crossing of Contralateral Retinal Axons at the Optic Chiasm Is Impaired in SoxC Mutants In Vivo

First, we investigated the involvement of SoxC TFs on axon outgrowth at E18.5 in vivo by deletion of SoxC genes at the transition between progenitor and postmitotic state by electroporation of *CAG-GFP* and *CAG-Cre* plasmids into $Sox4^{f/f}Sox11^{f/f}Sox12^{-/-}$ at E14.5. SoxC mutant GFP$^+$ cells remained in the progenitor zone below the RGC layer (Figure 4), and few axons extended into the optic nerve and into the optic chiasm (Figure S7).

We then examined the role of SoxC TFs in retinal axon guidance at the optic chiasm midline in vivo by deleting SoxC genes with greater temporal control. E14.5 $Sox4^{f/f}Sox11^{f/f}Sox12^{-/-}$ non-VT retina were electroporated in utero with *CAG-GFP* and $CAG-ER^{T2}CreER^{T2}$ plasmids and then injected intraperitoneally (i.p.) with 4OHT at E16 to delete SoxC genes in the electroporated RGCs. At the time of 4OHT injection, ~40% of GFP$^+$ cells in the WT and Sox mutant retina were Islet1/2$^+$ RGCs, and the axons of these cells projected into the optic nerve, but not as far as the optic chiasm (data not shown). *CAG-GFP* and $CAG-ER^{T2}CreER^{T2}$ plasmids were co-electroporated together at E14.5, and 4OHT was then injected at E16, and the efficiency of co-transfection was examined at E18.5. 93.6% ± 1.0% of

(G and H) Quantification of Islet1/2$^+$/GFP$^+$ cells (%) (G) and Ki67$^+$/GFP$^+$ cells (%) (H) in WT or $Sox4^{-/-}Sox11^{-/-}Sox12^{-/-}$ DT retinal cells cultured with control or DAPT (>370 of total GFP$^+$ cells counted for each condition; n = 4–5; one-way ANOVA).

(I) qRT-PCR measurements of *Hes5*, *Hes1*, and *Ccnd1* mRNAs of WT and $Sox4^{-/-}Sox11^{-/-}Sox12^{-/-}$ GFP$^+$ cells. n = 4; Student's t test.

See also Figures S3 and S4. Scale bars, 100 μm in (A); 10 μm in (C) and (F). *p < 0.05, **p < 0.01, ***p < 0.001; N.S., not significant.

Figure 4. Contralateral RGC Differentiation Is Impaired in SoxC Mutant Cells In Vivo

(A) Schema of in utero retinal electroporation of *CAG-GFP* and *CAG-Cre* plasmids into E14.5 WT or *Sox4$^{f/f}$Sox11$^{f/f}$Sox12$^{-/-}$* non-VT retina and analysis of RGC differentiation in central retina at E18.5.
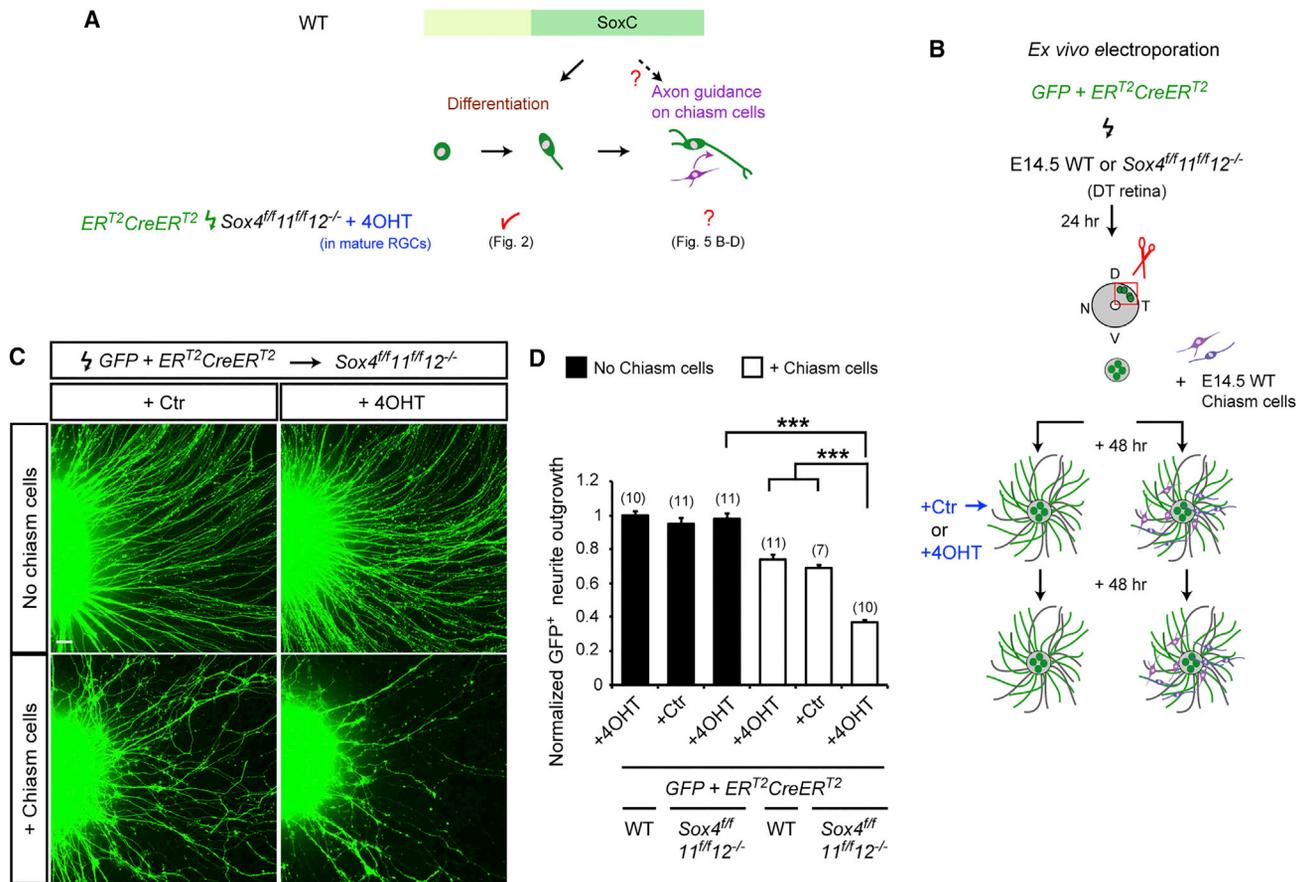
(B) Most E18.5 WT GFP$^+$ retinal cells have differentiated into Islet1/2$^+$ postmitotic RGCs (arrows in high magnification views), while many *Sox4$^{-/-}$Sox11$^{-/-}$Sox12$^{-/-}$* GFP$^+$ retinal cells remain as Ki67$^+$ progenitor cells (arrowheads).

(C and D) Quantification of Islet1/2$^+$/GFP$^+$ cells (%) (C) and Ki67$^+$/GFP$^+$ cells (%) (D) in WT, *Sox12$^{-/-}$*, and *Sox4$^{-/-}$Sox11$^{-/-}$Sox12$^{-/-}$* non-VT retina (>2,000 of total GFP$^+$ cells counted for each condition; n = 4–5; one-way ANOVA).

Non-VT, non-ventrotemporal. Scale bar, 20 μm. ***p < 0.001.

GFP$^+$ cells express Cre in nucleus (>350 of total GFP$^+$ cells counted, n = 3 embryos). We then analyzed the number of Islet1/2$^+$ RGCs and Ki67$^+$ progenitor cells in *Sox4$^{-/-}$Sox11$^{-/-}$Sox12$^{-/-}$* retina at E18.5 (two days post-4OHT injection) (Figures 6A–6C). In both WT and *Sox4$^{-/-}$Sox11$^{-/-}$Sox12$^{-/-}$* embryos, ~60% of GFP cells express Islet1/2 and ~12% of GFP cells express Ki67, indicating that mutant and WT retinae have differentiated similarly (Figures 6B and 6C).

Next, we analyzed axon projections in WT and *Sox4$^{-/-}$Sox11$^{-/-}$Sox12$^{-/-}$* RGCs at the optic chiasm midline at E18.5 (Figures 6D and 6E). The cells in central retina in both WT and mutant retina were electroporated, and thus almost all GFP$^+$ axons in WT embryos projected contralaterally. In contrast, in *Sox4$^{-/-}$Sox11$^{-/-}$Sox12$^{-/-}$* mice, GFP$^+$ RGC axons electroporated in central retina projected both ipsilaterally and contralaterally (Figure 6D). As indicated by the ipsilateral index analysis, a

Figure 5. SoxC TFs Are Important for Contralateral RGC Axon Outgrowth on Chiasm Cells

(A) Schema of hypothesis that SoxC TFs mediate axon guidance in response to signals from chiasm cells: after electroporation of $CAG\text{-}ER^{T2}CreER^{T2}$ into $Sox4^{f/f}Sox11^{f/f}Sox12^{-/-}$ retina, retinal explants are treated with 4OHT only after RGC outgrowth has occurred (B)–(D).

(B) Schema of ex vivo electroporation of $CAG\text{-}GFP$ and $CAG\text{-}ER^{T2}CreER^{T2}$ plasmids into E14.5 $Sox4^{f/f}Sox11^{f/f}Sox12^{-/-}$ DT retina to generate $Sox4^{-/-}Sox11^{-/-}Sox12^{-/-}$ GFP$^+$ neurons by 4OHT in differentiated RGCs with neurites.

(C) Representative images of $Sox12^{-/-}$ or $Sox4^{-/-}Sox11^{-/-}Sox12^{-/-}$ GFP$^+$ axon outgrowth with or without chiasm cells.

(D) Quantification of WT, $Sox12^{-/-}$, or $Sox4^{-/-}Sox11^{-/-}Sox12^{-/-}$ GFP$^+$ DT retinal outgrowth in the presence or absence of chiasm cells. n = number of explants for each condition; two-way ANOVA.

See also Figures S5 and S6. DT, dorsotemporal. Scale bars, 40 μm. ***p < 0.001.
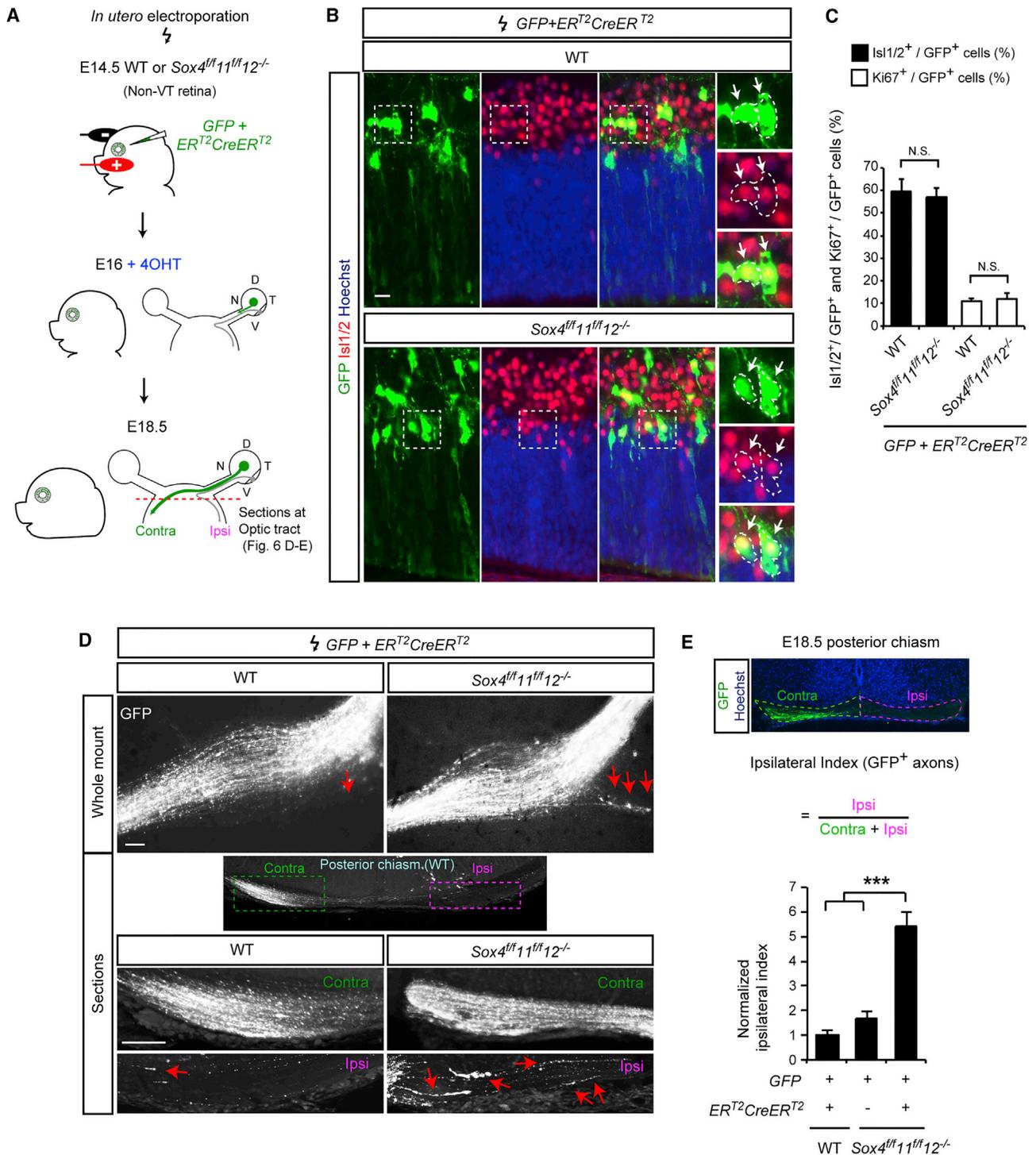
5-fold increase in the proportion of GFP$^+$ axons projecting ipsilaterally was observed in $Sox4^{-/-}Sox11^{-/-}Sox12^{-/-}$ mice compared with WT or $Sox12^{-/-}$ mice (Figure 6E).

We also examined whether $Sox4^{-/-}Sox11^{-/-}Sox12^{-/-}$ mutant contralateral and ipsilateral axons project to the superior colliculus (SC) and dorsal lateral geniculate nucleus (dLGN) compared with WT axons at E18.5 (Figure S8). Both WT and $Sox4^{-/-}Sox11^{-/-}Sox12^{-/-}$ RGC axons reached the borders of the contralateral SC and dLGN. In the WT, several ipsilateral axons could be detected at or near the chiasm midline (Figure 6D), but few were noted as far as the dLGN or SC (Figure S8). In contrast, in $Sox4^{-/-}Sox11^{-/-}Sox12^{-/-}$ mice, numerous ipsilateral axons were detected in the optic chiasm (Figure 6D) and in the optic tract outside the dLGN and the SC (Figure S8). As seen in the WT at E18 (Soares and Mason, 2015), the few transient ipsilateral axons from central retinal RGCs penetrate these targets ipsilaterally. Taken together, deletion of SoxC genes in

postmitotic RGCs led to an increased ipsilateral projection, and the aberrant ipsilateral axons can reach the borders of their targets in dLGN and SC but do not penetrate them. These data suggest that SoxC factors play a role in contralateral RGC differentiation as well as axon guidance at the optic chiasm midline.

SoxC TFs Regulate Plexin-A1 and NrCAM Expression in RGCs

Two possible molecular mechanisms could explain the aberrant projection of central retinal RGC axons ipsilaterally in SoxC mutants in which the SoxC TFs were ablated at E16.5–E18.5. First, axon guidance receptors in contralateral RGCs such as Plexin-A1, Nr-CAM, and Neuropilin1 (Erskine et al., 2011; Kuwajima et al., 2012) could be downregulated in the absence of SoxC genes. Alternatively (or in addition), the ipsilateral transcription factor Zic2 and/or the ipsilateral axon guidance receptor EphB1 (Herrera et al., 2003; Williams et al., 2003) could be

Figure 6. SoxC TFs Mediate Contralateral RGC Axon Projection at the Chiasm Midline

(A) Schema of in utero retinal electroporation of *CAG-GFP* and *CAG-ER^{T2}CreER^{T2}* plasmids into E14.5 WT or *Sox4$^{f/f}$Sox11$^{f/f}$Sox12$^{-/-}$* retina away from VT retina, injection of 4OHT i.p. at E16, and analysis of RGC differentiation and retinal axon decussation at E18.5.

(B) Most E18.5 WT GFP$^+$ retinal cells and *Sox4$^{-/-}$Sox11$^{-/-}$Sox12$^{-/-}$* GFP$^+$ retinal cells have differentiated to Islet1/2$^+$ postmitotic RGCs (arrows).

(C) Quantification of Islet1/2$^+$ and Ki67$^+$/GFP$^+$ cells (%) in WT and *Sox4$^{-/-}$Sox11$^{-/-}$Sox12$^{-/-}$* retina (>870 of total GFP$^+$ cells counted for each condition; n = 3; two-way ANOVA).

(legend continued on next page)

ectopically induced in RGCs in the absence of SoxC TFs. We therefore examined the expression of *Plexin-A1*, *Nr-CAM*, *Neuropilin1*, and *EphB1* mRNA, and Zic2 protein in E18.5 $Sox4^{-/-}Sox11^{-/-}Sox12^{-/-}$ retina in vivo after in utero electroporation of *CAG-GFP* and *CAG-ER^T2^CreER^T2^* at E14.5 and treatment with 4OHT at E16 (Figures 7A and 7B). $Sox4^{-/-}Sox11^{-/-}Sox12^{-/-}$ GFP+ RGCs failed to express *Plexin-A1* and *Nr-CAM* mRNAs compared to WT GFP+ cells, although *Neuropilin1* mRNA was detected in SoxC mutant cells (Figure 7A). Zic2 protein and *EphB1* mRNA were not ectopically induced in $Sox4^{-/-}Sox11^{-/-}Sox12^{-/-}$ GFP+ RGCs in non-VT retina (Figure 7B).

We next examined whether *Plexna1* (encoding Plexin-A1) and *Nrcam* (encoding Nr-CAM) are direct targets of SoxC TFs (Figures 7C–7F). We searched for conserved regions among binocular species within the 5′ non-coding regions (−1 to approximately −5,000) of *Plexna1* and *Nrcam* using the UCSC Genome Browser and, using TESS and PROMO, predicted TF binding. We found that putative regulatory non-coding regions of *Plexna1* and *Nrcam* contain pan-Sox binding sites C(T/A)TTG(T/A)(T/A) (Bhattaram et al., 2010; Messeguer et al., 2002; Schug, 2008). We made luciferase-based reporter constructs containing Sox binding sites for *Plexna1* and *Nrcam* non-coding regions (Figure 7C) and examined whether SoxC TFs modulate transcriptional activity of *Plexna1* and *Nrcam* promoters in HEK293 cells (Figure 7D) and in SoxC mutant DT retinal cells in vitro (Figure 7E). Ectopic expression of SoxC TFs upregulated transcriptional activity of both promoters in HEK293 cells (Figure 7D). Endogenous SoxC TFs upregulate the transcriptional activity of *Plexna1* and *Nrcam* promoters in 3-day cultures compared to 1-day cultures of WT DT retina. In contrast, transcriptional activation of neither promoter could be detected in 3-day DT cultures after deletion of SoxC genes in postmitotic RGCs. The activity was slightly elevated in 3-day cultures of WT VT retina (Figure 7E).

Finally, binding of SoxC TFs to *Plexna1* and *Nrcam* promoters was analyzed by chromatin immunoprecipitation (ChIP) (Figure 7F). An enrichment of predicted DNA on *Plexna1* and *Nrcam* promoters was detected with anti-FLAG antibody after electroporation of FLAG-tagged Sox4, FLAG-tagged Sox11, or FLAG-tagged Sox12 construct into DT retina compared with control IgG or FLAG-antibody after electroporation of empty vector.

Together, these data indicate that SoxC TFs bind to the promoters of *Plexna1* and *Nrcam* and regulate their expression, in contralateral RGCs.

DISCUSSION

Mechanisms of contralateral RGC growth and guidance during formation of the binocular visual circuit are poorly understood compared with the directives for ipsilateral RGC growth and guidance. Through an in silico search, we identified the SoxC transcription factors as candidates that direct the contralateral RGC

projection during optic chiasm formation, through regulation of RGC differentiation and expression of axon guidance receptors Plexin-A1 and Nr-CAM. In this study, inactivation of SoxC TFs at two specific time points in RGC development, i.e., during RGC proliferation and axon guidance, allowed us to reveal a dual function for SoxC TFs that actively contributes to contralateral RGC differentiation and growth at the optic chiasm (Figure 8).

SoxC TFs Regulate Differentiation of RGCs that Project Contralaterally

TFs crucial for RGC cell-fate specification have been identified (Wang and Harris, 2005; Xiang, 2013). The subsequent differentiation of postmitotic RGCs is mediated by various TFs in monocular and binocular species (Kanekar et al., 1997; Wu et al., 2015). However, TFs selectively mediating contralateral as opposed to ipsilateral RGC cell fate and differentiation have not been previously identified. Our study demonstrates that SoxC TFs are necessary for contralateral RGC differentiation at the transition between progenitor and the early postmitotic state (Figures 2 and 4), although RGCs in VT retina during the period of ipsilateral RGC genesis from E14 to E17 do not appear to require SoxC TFs. However, from E17.5 to P0, SoxC genes are expressed within VT retina, where contralateral RGCs also reside in this late period, implying that SoxC TFs may also mediate later-born contralateral RGC differentiation from E17.5 onward.

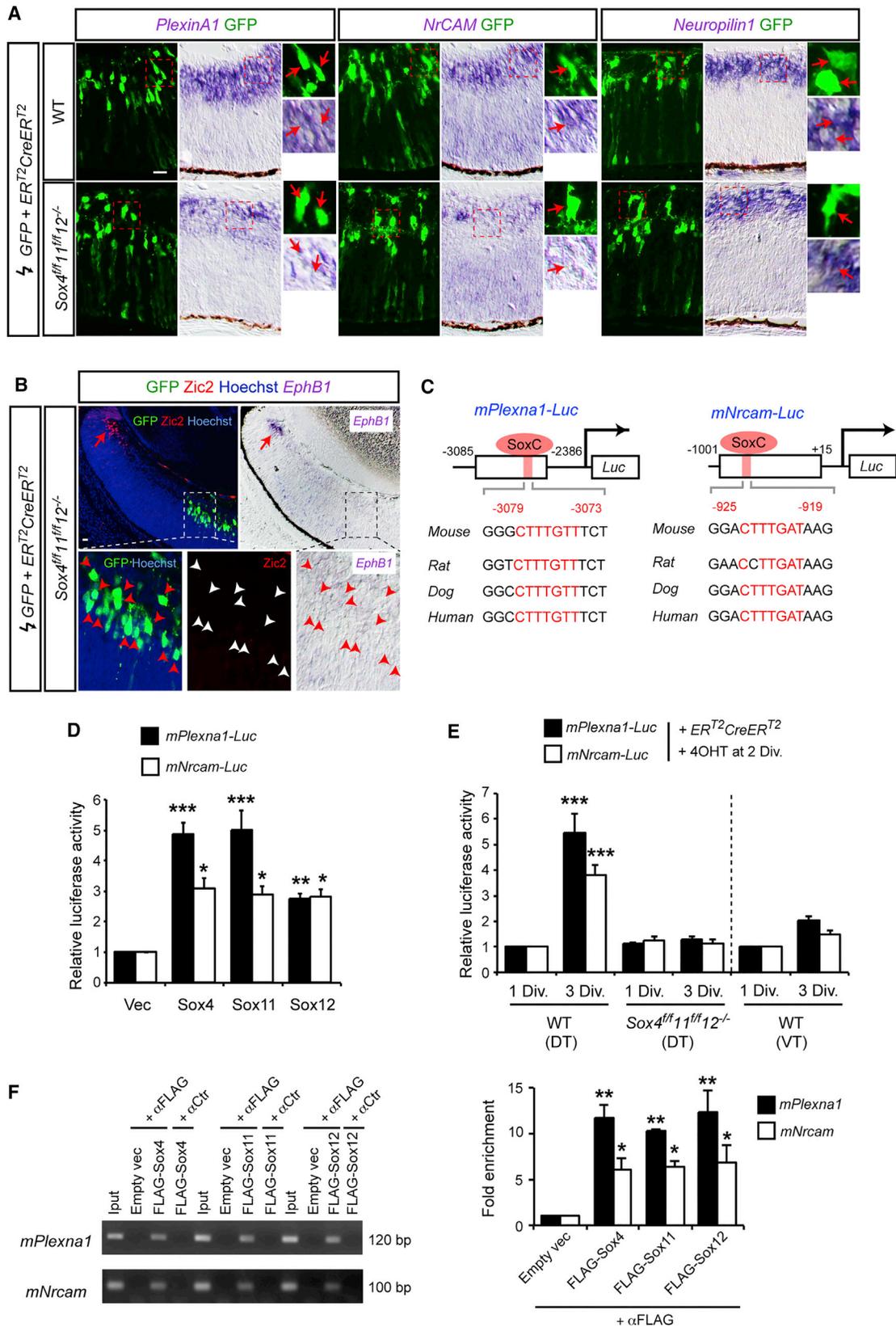### SoxC TFs Stimulate Contralateral RGC Differentiation by Antagonizing the Notch Signaling Pathway

Notch and its downstream effector, the bHLH transcription factor Hes, are important for retinal morphogenesis, progenitor cell maintenance, cell-fate determination, and specification in the retina (Bao and Cepko, 1997; Henrique et al., 1997; Jadhav et al., 2006; Maurer et al., 2014; Mizeracka et al., 2013; Nelson et al., 2006; Ohtsuka et al., 1999). Sox4 and Sox11 regulate neuronal differentiation in the developing cortex through regulating their targets NeuroD1 and Tbr2 (Chen et al., 2015). Our study is the first to show that the Notch1-Hes5 signaling pathway is important for maintaining the progenitor state specifically of contralateral retinal progenitors and that antagonistic interactions between Notch-Hes5 and SoxC TFs influence the balance between cell proliferation and RGC differentiation in regions of the retina giving rise to contralateral RGCs (Figure 3).

The individual SoxC TFs are not functionally equivalent: Sox11 and 12 strongly antagonize Notch-induced transcriptional activity of Hes5, but Sox4 only moderately antagonizes Notch activity, although $Sox4^{-/-}$ and $Sox11^{-/-}$ single mutant retina shows more severe defects in RGC differentiation than $Sox12^{-/-}$ retina, which displays normal RGC differentiation (Figures 2C and 2D). In fact, $Sox4^{-/-}Sox11^{-/-}Sox12^{-/-}$ triple mutant DT retina has fewer RGCs than in the $Sox4^{-/-}$ or $Sox11^{-/-}$ single mutant or $Sox4^{-/-}Sox11^{-/-}$ double mutants (Figure 2E). In other systems, $Sox4^{-/-}Sox11^{-/-}Sox12^{-/-}$ triple mutants have a thinner neural
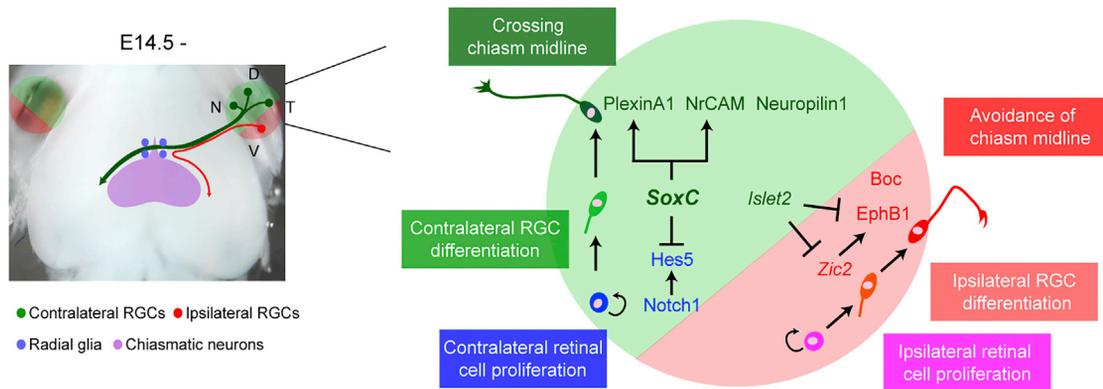
(D) A whole mount view of the GFP+ axon projection from electroporated retina to the optic chiasm, and 300 μm chiasm sections after tissue clearing with *Clear^T2^* (Sections) in WT and $Sox4^{-/-}Sox11^{-/-}Sox12^{-/-}$ mutants. Arrows indicate axons projecting ipsilaterally.

(E) Quantification of GFP+ ipsilateral projection from WT, $Sox12^{-/-}$, or $Sox4^{-/-}Sox11^{-/-}Sox12^{-/-}$ non-VT retina. n = 4–6; one-way ANOVA. Schematic shows the measurement of pixel intensity of contralateral and ipsilateral optic tracts and the calculation to obtain an ipsilateral index.

See also Figures S7 and S8. Non-VT, non-ventrotemporal. Scale bars, 20 μm in (B); 100 μm in (D). ***$p < 0.001$; N.S., not significant.

(legend on next page)

Figure 8. Functions of SoxC TFs in Contralateral Retina

SoxC TFs in non-VT retina promote contralateral RGC differentiation and axon guidance at the optic chiasm midline through interactions with their molecular targets, *Hes5*, *Plexna1*, and *Nrcam*. In contrast, Zic2-EphB1 interactions mediate ipsilateral RGC axon projection and are repressed by Isl2, a TF for contralateral RGC axon guidance (Pak et al., 2004) and influenced by a cell adhesion molecule, Boc (Fabre et al., 2010; Sánchez-Arrones et al., 2013).

tube compared with $Sox4^{-/-}Sox11^{-/-}$ mutants (Bhattaram et al., 2010). Loss of function in $Sox12^{-/-}$ retina might be compensated through increased expression of *Sox4* and *Sox11* in the retina, as previously shown in the brain and spinal cord (Hoser et al., 2008). Therefore, loss of *Sox12* function could be adjusted by upregulation of Sox4 and 11 expression and/or enrichment of Sox4 and 11 on the target promoter region.

SoxC TFs and Hes5 do not appear to be involved in ipsilateral RGC differentiation, even though they are expressed in progenitors in VT retina (Figures 2C, S3, and S4). How is proliferation and differentiation of ipsilateral RGCs, which are situated exclusively in VT retina, regulated? Most recently, we have identified Cyclin D2 as a regulator of cell-cycle progression and exit in VT retina during the production of Zic2$^+$ RGCs (Marcucci et al., 2016; Wang et al., 2016). As overexpression of Hes5 in VT retina has no effect on RGC differentiation, contralateral and ipsilateral RGC differentiation may be mediated by distinct molecules and/or downstream signals of Hes5.

Regulation of the Contralateral RGC Projection by SoxC TFs Is Independent of Zic2

How are the contralateral and ipsilateral retinal projections encoded in binocular species? TFs responsible for contralateral RGC specification might suppress expression of TFs for ipsilateral RGC specification, or vice versa. SoxC TFs show expression patterns complementary to those of Zic2, but Zic2 expression was not detected in SoxC-deficient RGCs (Figure 7B). Moreover, overexpression of Zic2 in contralateral retina does not affect RGC differentiation even though axon outgrowth is perturbed (García-Frigola et al., 2008). These data suggest that SoxC TFs do not affect Zic2 expression (Figure 7).

Interestingly, loss of Islet2, which is normally expressed in a subset of contralateral RGCs, leads to an increased number of Zic2$^+$ RGCs in VT retina and a concomitantly increased ipsilateral projection (Pak et al., 2004). Taken together, while a Islet2-Zic2 cross repression appears to participate in the designation of ipsilateral and contralateral RGCs, SoxC TFs do not appear to engage with the Zic2 pathway during binocular visual circuit formation (Figure 8).

Transcriptional Code for the Contralateral RGC Projection: SoxC TFs Regulate Axon Guidance Receptor Expression

TFs selectively regulate expression of axon guidance receptors and ligands and contribute to proper neural connectivity in the nervous system (Butler and Tear, 2007; Erskine and Herrera, 2014; Polleux et al., 2007). Our study has shown that SoxC TFs bind to the promoter regions of *Plexna1* and *Nrcam* and regulate their expression levels in contralateral retina (Figure 7). While $Nr\text{-}CAM^{-/-}$ and $Islet2^{-/-}$ single mutants display the same

Figure 7. *Plexna1* and *Nrcam* Are Targets of SoxC TFs

(A and B) Expression of *Plexin-A1*, *Nr-CAM*, and *Neuropilin1* mRNAs (A) and Zic2 protein and *EphB1* mRNA (B) in E18.5 WT or $Sox4^{-/-}Sox11^{-/-}Sox12^{-/-}$ GFP$^+$ cells in central retina. Note that $Sox4^{-/-}Sox11^{-/-}Sox12^{-/-}$ display little expression of *Plexin-A1* and *Nr-CAM* mRNAs, while *Neuropilin1* mRNA is unaffected (arrows) (A). Zic2 protein and *EphB1* mRNA were detected in VT retina (arrows), but not in $Sox4^{-/-}Sox11^{-/-}Sox12^{-/-}$ GFP$^+$ cells (arrowheads) (B).

(C) Conserved Sox-binding sites in *Plexna1* and *Nrcam* 5′ non-coding region among binocular species and construction of luciferase-based reporter vectors.

(D and E) Luciferase assay: HEK293 cells were transfected with combinations of expression vectors for SoxC (4, 11, 12) (3.6 μg) with reporter vector (0.3 μg) and a *Renilla* luciferase construct (0.03 μg) (D). 0.5 μL of DNA solution of *GFP* (0.5 μg/μl), $ER^{T2}CreER^{T2}$ (2.0 μg/μL), and reporter vector (0.5 μg/μL) with a *Renilla* luciferase construct (0.05 μg/μL) was electroporated into E14.5 WT or $Sox4^{f/f}Sox11^{f/f}Sox12^{-/-}$ contralateral (DT) or ipsilateral (VT) retina. Dissociated retinal cells were cultured for 1 or 3 days or incubated with 4OHT for 1 day and analyzed (E). Data are presented as fold change in relative luciferase activity normalized to the mean of empty vector (Vec) (D) or WT (WT, 1 Div.) (E). n = 3–5; two-way ANOVA (D) and three-way ANOVA (E).

(F) Chip assay in DT retina, which was electroporated with FLAG-tagged Sox4, Sox11, Sox12, or empty vector and cultured. The *Plexna1* and *Nrcam* promoter sequences were amplified by PCR using input DNA (1% of total sample) and total immunoprecipitated DNA with FLAG antibody. The fold enrichment was quantified after ChIP assay with FLAG antibody. n = 3–5; two-way ANOVA.

DT, dorsotemporal; VT, ventrotemporal. Scale bars, 20 μm. *p < 0.05, **p < 0.01, ***p < 0.001.

defects in the contralateral projection at E18–P0 (Pak et al., 2004; Williams et al., 2006), Islet2 fails to activate transcriptional activities of *Nrcam* promoter regions including Islet2 binding sites by luciferase reporter assay (data not shown).

What molecular mechanisms lead to an induction of an ipsilateral projection from non-VT retina in SoxC$^{-/-}$ embryos? Plexin-A1 and Nr-CAM expressed in contralateral RGCs serve as receptors for semaphorin6D, Plexin-A1, and Nr-CAM, which are expressed at the optic chiasm midline and facilitate contralateral RGC axon midline crossing (Kuwajima et al., 2012). Therefore, downregulation of functional receptors, Plexin-A1, and Nr-CAM in SoxC$^{-/-}$ mutant retina may lead to a reduction in retinal axon midline crossing in response to growth-permissive signals from chiasm cells (Figure 6). Moreover, the inhibitory chiasmatic environment would induce SoxC$^{-/-}$ mutant RGC axons from central retina to avoid the midline, leading to an increase in ipsilateral axons extending to the LGN and SC (Figure S8). However, the maintenance of the contralateral projection in SoxC mutant RGC axons may be due to the continued expression of *Neuropilin1* (Erskine et al., 2011) (Figure 7A). Thus, depletion of *Neuropilin1* in SoxC mutant contralateral retina would be predicted to lead to additional increased ipsilateral projection in SoxC mutants. Moreover, *Cre-loxP* recombination in the electroporated RGCs could have occurred after many of their axons had passed through the chiasm.

In summary, we have elucidated the function of SoxC TFs in RGCs that project contralaterally, through controlling distinct targets for their differentiation and axon guidance. Further investigation is needed to determine whether SoxC TFs control expression of these target genes for RGC differentiation and axon guidance simultaneously or sequentially, whether SoxC TFs are also involved in more distal phases, in axon targeting and RGC axon regeneration, and how the regulation of ipsilateral RGC differentiation intersects with contralateral RGC differentiation.

STAR★METHODS

Detailed methods are provided in the online version of this paper and include the following:

- KEY RESOURCES TABLE
- CONTACT FOR REAGENT AND RESOURCE SHARING
- EXPERIMENTAL MODEL AND SUBJECT DETAILS
  - Animals
- METHOD DETAILS
  - In situ hybridization and Immunohistochemistry
  - Electroporation
  - Retinal cell cultures and analysis
  - In vivo analysis
  - Luciferase assay
  - ChIP assay
  - qRT-PCR
- QUANTIFICATION AND STATISTICAL ANALYSIS

SUPPLEMENTAL INFORMATION

Supplemental Information includes eight figures and can be found with this article online at http://dx.doi.org/10.1016/j.neuron.2017.01.029.

AUTHOR CONTRIBUTIONS

ACKNOWLEDGMENTS

REFERENCES

Akazawa, C., Sasai, Y., Nakanishi, S., and Kageyama, R. (1992). Molecular characterization of a rat negative regulator with a basic helix-loop-helix structure predominantly expressed in the developing nervous system. J. Biol. Chem. *267*, 21879–21885.

Bao, Z.Z., and Cepko, C.L. (1997). The expression and function of Notch pathway genes in the developing rat eye. J. Neurosci. *17*, 1425–1434.

Bélanger, M.C., Robert, B., and Cayouette, M. (2017). Msx1-Positive Progenitors in the Retinal Ciliary Margin Give Rise to Both Neural and Non-neural Progenies in Mammals. Dev Cell *40*, 137–150.

Bhansali, P., Rayport, I., Rebsam, A., and Mason, C. (2014). Delayed neurogenesis leads to altered specification of ventrotemporal retinal ganglion cells in albino mice. Neural Dev. *9*, 11.

Bhattaram, P., Penzo-Méndez, A., Sock, E., Colmenares, C., Kaneko, K.J., Vassilev, A., Depamphilis, M.L., Wegner, M., and Lefebvre, V. (2010). Organogenesis relies on SoxC transcription factors for the survival of neural and mesenchymal progenitors. Nat. Commun. *1*, 9.

Brown, L.Y., Kottmann, A.H., and Brown, S. (2003). Immunolocalization of Zic2 expression in the developing mouse forebrain. Gene Expr. Patterns *3*, 361–367.

Butler, S.J., and Tear, G. (2007). Getting axons onto the right path: the role of transcription factors in axon guidance. Development *134*, 439–448.

Chen, C., Lee, G.A., Pourmorady, A., Sock, E., and Donoghue, M.J. (2015). Orchestration of Neuronal Differentiation and Progenitor Pool Expansion in the Developing Cortex by SoxC Genes. J. Neurosci. *35*, 10629–10642.

Das, G., Choi, Y., Sicinski, P., and Levine, E.M. (2009). Cyclin D1 fine-tunes the neurogenic output of embryonic retinal progenitor cells. Neural Dev. *4*, 15.

Dodd, J., Morton, S.B., Karagogeos, D., Yamamoto, M., and Jessell, T.M. (1988). Spatial regulation of axonal glycoprotein expression on subsets of embryonic spinal neurons. Neuron *1*, 105–116.

Dy, P., Penzo-Méndez, A., Wang, H., Pedraza, C.E., Macklin, W.B., and Lefebvre, V. (2008). The three SoxC proteins–Sox4, Sox11 and Sox12–exhibit overlapping expression patterns and molecular properties. Nucleic Acids Res. *36*, 3101–3117.

Erskine, L., and Herrera, E. (2014). Connecting the retina to the brain. ASN Neuro *6*, 6.

CellPress

Erskine, L., Reijntjes, S., Pratt, T., Denti, L., Schwarz, Q., Vieira, J.M., Alakakone, B., Shewan, D., and Ruhrberg, C. (2011). VEGF signaling through neuropilin 1 guides commissural axon crossing at the optic chiasm. Neuron 70, 951–965.

Fabre, P.J., Shimogori, T., and Charron, F. (2010). Segregation of ipsilateral retinal ganglion cell axons at the optic chiasm requires the Shh receptor Boc. J. Neurosci. 30, 266–275.

García-Frigola, C., and Herrera, E. (2010). Zic2 regulates the expression of Sert to modulate eye-specific refinement at the visual targets. EMBO J. 29, 3170–3183.

Garcia-Frigola, C., Carreres, M.I., Vegar, C., and Herrera, E. (2007). Gene delivery into mouse retinal ganglion cells by in utero electroporation. BMC Dev. Biol. 7, 103.

García-Frigola, C., Carreres, M.I., Vegar, C., Mason, C., and Herrera, E. (2008). Zic2 promotes axonal divergence at the optic chiasm midline by EphB1-dependent and -independent mechanisms. Development 135, 1833–1841.

Henrique, D., Hirsinger, E., Adam, J., Le Roux, I., Pourquié, O., Ish-Horowicz, D., and Lewis, J. (1997). Maintenance of neuroepithelial progenitor cells by Delta-Notch signalling in the embryonic chick retina. Curr. Biol. 7, 661–670.

Herrera, E., Brown, L., Aruga, J., Rachel, R.A., Dolen, G., Mikoshiba, K., Brown, S., and Mason, C.A. (2003). Zic2 patterns binocular vision by specifying the uncrossed retinal projection. Cell 114, 545–557.

Hoser, M., Potzner, M.R., Koch, J.M., Bösl, M.R., Wegner, M., and Sock, E. (2008). Sox12 deletion in the mouse reveals nonreciprocal redundancy with the related Sox4 and Sox11 transcription factors. Mol. Cell. Biol. 28, 4675–4687.

Huang, H.Y., Cheng, Y.Y., Liao, W.C., Tien, Y.W., Yang, C.H., Hsu, S.M., and Huang, P.H. (2012). SOX4 transcriptionally regulates multiple SEMA3/plexin family members and promotes tumor growth in pancreatic cancer. PLoS ONE 7, e48637.

Jadhav, A.P., Cho, S.H., and Cepko, C.L. (2006). Notch activity permits retinal cells to progress through multiple progenitor states and acquire a stem cell property. Proc. Natl. Acad. Sci. USA 103, 18998–19003.

Jessell, T.M. (2000). Neuronal specification in the spinal cord: inductive signals and transcriptional codes. Nat. Rev. Genet. 1, 20–29.

Jiang, Y., Ding, Q., Xie, X., Libby, R.T., Lefebvre, V., and Gan, L. (2013). Transcription factors SOX4 and SOX11 function redundantly to regulate the development of mouse retinal ganglion cells. J. Biol. Chem. 288, 18429–18438.

Kanekar, S., Perron, M., Dorsky, R., Harris, W.A., Jan, L.Y., Jan, Y.N., and Vetter, M.L. (1997). Xath5 participates in a network of bHLH genes in the developing Xenopus retina. Neuron 19, 981–994.

Kothapalli, D., Zhao, L., Hawthorne, E.A., Cheng, Y., Lee, E., Puré, E., and Assoian, R.K. (2007). Hyaluronan and CD44 antagonize mitogen-dependent cyclin D1 expression in mesenchymal cells. J. Cell Biol. 176, 535–544.

Kurita, M., Kuwajima, T., Nishimura, I., and Yoshikawa, K. (2006). Necdin downregulates CDC2 expression to attenuate neuronal apoptosis. J. Neurosci. 26, 12003–12013.

Kuwajima, T., Yoshida, Y., Takegahara, N., Petros, T.J., Kumanogoh, A., Jessell, T.M., Sakurai, T., and Mason, C. (2012). Optic chiasm presentation of Semaphorin6D in the context of Plexin-A1 and Nr-CAM promotes retinal axon midline crossing. Neuron 74, 676–690.

Kuwajima, T., Sitko, A.A., Bhansali, P., Jurgens, C., Guido, W., and Mason, C. (2013). ClearT: a detergent- and solvent-free clearing method for neuronal and non-neuronal tissue. Development 140, 1364–1368.

Lee, R., Petros, T.J., and Mason, C.A. (2008). Zic2 regulates retinal ganglion cell axon avoidance of ephrinB2 through inducing expression of the guidance receptor EphB1. J. Neurosci. 28, 5910–5919.

Marcucci, F., Murcia-Belmonte, V., Wang, Q., Coca, Y., Ferreiro-Galve, S., Kuwajima, T., Khalid, S., Ross, M.E., Mason, C., and Herrera, E. (2016). The Ciliary Margin Zone of the Mammalian Retina Generates Retinal Ganglion Cells. Cell Rep. 17, 3153–3164.

Matsuda, T., and Cepko, C.L. (2007). Controlled expression of transgenes introduced by in vivo electroporation. Proc. Natl. Acad. Sci. USA 104, 1027–1032.

Matsuda, S., Kuwako, K., Okano, H.J., Tsutsumi, S., Aburatani, H., Saga, Y., Matsuzaki, Y., Akaike, A., Sugimoto, H., and Okano, H. (2012). Sox21 promotes hippocampal adult neurogenesis via the transcriptional repression of the Hes5 gene. J. Neurosci. 32, 12543–12557.

Maurer, K.A., Riesenberg, A.N., and Brown, N.L. (2014). Notch signaling differentially regulates Atoh7 and Neurog2 in the distal mouse retina. Development 141, 3243–3254.

Messeguer, X., Escudero, R., Farré, D., Núñez, O., Martínez, J., and Albà, M.M. (2002). PROMO: detection of known transcription regulatory elements using species-tailored searches. Bioinformatics 18, 333–334.

Mizeracka, K., DeMaso, C.R., and Cepko, C.L. (2013). Notch1 is required in newly postmitotic cells to inhibit the rod photoreceptor fate. Development 140, 3188–3197.

Nelson, B.R., Gumuscu, B., Hartman, B.H., and Reh, T.A. (2006). Notch activity is downregulated just prior to retinal ganglion cell differentiation. Dev. Neurosci. 28, 128–141.

Nelson, B.R., Hartman, B.H., Georgi, S.A., Lan, M.S., and Reh, T.A. (2007). Transient inactivation of Notch signaling synchronizes differentiation of neural progenitor cells. Dev. Biol. 304, 479–498.

Ohtsuka, T., Ishibashi, M., Gradwohl, G., Nakanishi, S., Guillemot, F., and Kageyama, R. (1999). Hes1 and Hes5 as notch effectors in mammalian neuronal differentiation. EMBO J. 18, 2196–2207.

Pak, W., Hindges, R., Lim, Y.S., Pfaff, S.L., and O'Leary, D.D. (2004). Magnitude of binocular vision controlled by islet-2 repression of a genetic program that specifies laterality of retinal axon pathfinding. Cell 119, 567–578.

Pan, L., Deng, M., Xie, X., and Gan, L. (2008). ISL1 and BRN3B co-regulate the differentiation of murine retinal ganglion cells. Development 135, 1981–1990.

Penzo-Méndez, A., Dy, P., Pallavi, B., and Lefebvre, V. (2007). Generation of mice harboring a Sox4 conditional null allele. Genesis 45, 776–780.

Petros, T.J., Rebsam, A., and Mason, C.A. (2008). Retinal axon growth at the optic chiasm: to cross or not to cross. Annu. Rev. Neurosci. 31, 295–315.

Petros, T.J., Shrestha, B.R., and Mason, C. (2009). Specificity and sufficiency of EphB1 in driving the ipsilateral retinal projection. J. Neurosci. 29, 3463–3474.

Polleux, F., Ince-Dunn, G., and Ghosh, A. (2007). Transcriptional regulation of vertebrate axon guidance and synapse formation. Nat. Rev. Neurosci. 8, 331–340.

Quina, L.A., Pak, W., Lanier, J., Banwait, P., Gratwick, K., Liu, Y., Velasquez, T., O'Leary, D.D., Goulding, M., and Turner, E.E. (2005). Brn3a-expressing retinal ganglion cells project specifically to thalamocortical and collicular visual pathways. J. Neurosci. 25, 11595–11604.

Reaume, A.G., Conlon, R.A., Zirngibl, R., Yamaguchi, T.P., and Rossant, J. (1992). Expression analysis of a Notch homologue in the mouse embryo. Dev. Biol. 154, 377–387.

Sánchez-Arrones, L., Nieto-Lopez, F., Sánchez-Camacho, C., Carreres, M.I., Herrera, E., Okada, A., and Bovolenta, P. (2013). Shh/Boc signaling is required for sustained generation of ipsilateral projecting ganglion cells in the mouse retina. J. Neurosci. 33, 8596–8607.

Schug, J. (2008). Using TESS to predict transcription factor binding sites in DNA sequence. Curr. Protoc. Bioinformatics Chapter 2, 6.

Shim, S., Kwan, K.Y., Li, M., Lefebvre, V., and Sestan, N. (2012). Cis-regulatory control of corticospinal system development and evolution. Nature 486, 74–79.

Soares, C.A., and Mason, C.A. (2015). Transient ipsilateral retinal ganglion cell projections to the brain: Extent, targeting, and disappearance. Dev. Neurobiol. 75, 1385–1401.

Tiberi, L., van den Ameele, J., Dimidschstein, J., Piccirilli, J., Gall, D., Herpoel, A., Bilheu, A., Bonnefont, J., Iacovino, M., Kyba, M., et al. (2012). BCL6

controls neurogenesis through Sirt1-dependent epigenetic repression of selective Notch targets. Nat. Neurosci. *15*, 1627–1635.

Tsuchida, T., Ensini, M., Morton, S.B., Baldassare, M., Edlund, T., Jessell, T.M., and Pfaff, S.L. (1994). Topographic organization of embryonic motor neurons defined by expression of LIM homeobox genes. Cell *79*, 957–970.

Usui, A., Mochizuki, Y., Iida, A., Miyauchi, E., Satoh, S., Sock, E., Nakauchi, H., Aburatani, H., Murakami, A., Wegner, M., and Watanabe, S. (2013). The early retinal progenitor-expressed gene Sox11 regulates the timing of the differentiation of retinal cells. Development *140*, 740–750.

Wang, J.C., and Harris, W.A. (2005). The role of combinational coding by homeodomain and bHLH transcription factors in retinal cell fate specification. Dev. Biol. *285*, 101–115.

Wang, L.C., Rachel, R.A., Marcus, R.C., and Mason, C.A. (1996). Chemosuppression of retinal axon growth by the mouse optic chiasm. Neuron *17*, 849–862.

Wang, Q., Marcucci, F., Cerullo, I., and Mason, C. (2016). Ipsilateral and Contralateral Retinal Ganglion Cells Express Distinct Genes during Decussation at the Optic Chiasm. eNeuro *3*, ENEURO.0169-16.2016.

Williams, S.E., Mann, F., Erskine, L., Sakurai, T., Wei, S., Rossi, D.J., Gale, N.W., Holt, C.E., Mason, C.A., and Henkemeyer, M. (2003). Ephrin-B2 and EphB1 mediate retinal axon divergence at the optic chiasm. Neuron *39*, 919–935.

Williams, S.E., Grumet, M., Colman, D.R., Henkemeyer, M., Mason, C.A., and Sakurai, T. (2006). A role for Nr-CAM in the patterning of binocular visual pathways. Neuron *50*, 535–547.

Wong, A.W., Brickey, W.J., Taxman, D.J., van Deventer, H.W., Reed, W., Gao, J.X., Zheng, P., Liu, Y., Li, P., Blum, J.S., et al. (2003). CIITA-regulated plexin-A1 affects T-cell-dendritic cell interactions. Nat. Immunol. *4*, 891–898.

Wu, F., Kaczynski, T.J., Sethuramanujam, S., Li, R., Jain, V., Slaughter, M., and Mu, X. (2015). Two transcription factors, Pou4f2 and Isl1, are sufficient to specify the retinal ganglion cell fate. Proc. Natl. Acad. Sci. USA *112*, E1559–E1568.

Xiang, M. (2013). Intrinsic control of mammalian retinogenesis. Cell. Mol. Life Sci. *70*, 2519–2532.

Yoshida, Y., Han, B., Mendelsohn, M., and Jessell, T.M. (2006). PlexinA1 signaling directs the segregation of proprioceptive sensory axons in the developing spinal cord. Neuron *52*, 775–788.

CellPress

STAR★METHODS

KEY RESOURCES TABLE

REAGENT or RESOURCE	SOURCE	IDENTIFIER
Antibodies		
Chicken polyclonal anti-GFP	Abcam	Cat#ab13970; RRID: AB_300798
Rabbit polyclonal anti-GFP	Abcam	Cat#ab6556; RRID: AB_305564
Mouse monoclonal anti-Islet1/2 (4D5)	Gift of S. Morton and T. Jessell (University of Columbia); Tsuchida et al., 1994; Bhansali et al., 2014	RRID: AB_528173
Rabbit polyclonal anti-Ki67	EMD Millipore	Cat#AB9260; RRID: AB_2142366
Rabbit polyclonal anti-Zic2	Gift of S. Brown (University of Vermont); Brown et al., 2003; Herrera et al., 2003; see also Anti-Zic2 antibody, EMD Millipore (Cat# AB15392; RRID: AB_19977437)	RRID: AB_2315623
Mouse monoclonal anti-Cre	Abcam	Cat#ab24607; RRID: AB_448179
Mouse monoclonal anti-Brn3a (5A3.2)	EMD Millipore	Cat#MAB1585; RRID: AB_94166
Mouse monoclonal anti-neurofilament (2H3)	Gift of S. Morton and T. Jessell (University of Columbia); Dodd et al., 1988; Petros et al., 2009	RRID: AB_531793
Mouse monoclonal anti-Flag	Sigma-Aldrich	Cat#F1804; RRID: AB_262044
Goat anti-Chicken IgG Alexa Fluor 488	Thermo Fisher	Cat#A-11039; RRID: AB_2534096
Donkey anti-Rabbit IgG Alexa Fluor 488	Thermo Fisher	Cat#A-21206; RRID: AB_2535792
Goat anti-mouse IgG Cy3	Jackson ImmunoResearch	Cat#111-165-146
Goat anti-Rabbit IgG Cy3	Jackson ImmunoResearch	Cat#111-165-144; RRID: AB_2338006
Hoechst33258	Thermo Fisher	Cat#H3569
Chemicals, Peptides, and Recombinant Proteins		
DAPT	Sigma-Aldrich	Cat#D5942
(Z)-4-Hydoxytamoxifen	Sigma-Aldrich	Cat#H7904
Laminin	Thermo Fisher	Cat#23017015
Poly-L-ornithine solution	Sigma-Aldrich	Cat#P4957
Methylcellulose	Sigma-Aldrich	Cat#M0512
Critical Commercial Assays		
RNAqueous-Micro Total RNA Isolation Kit	Thermo Fisher	Cat#AM1931
Power SYBR Green PCR Master Mix	Thermo Fisher	Cat#4367659
Dual-Luciferase Reporter Assay System	Promega	Cat#E1910
HNPP Fluorescent Detection Kit	Sigma-Aldrich	Cat#11758888001
Experimental Models: Cell Lines		
HEK293 cells	Sigma-Aldrich	Cat#85120602
Experimental Models: Organisms/Strains		
Mouse model: Sox4$^{fl/fl}$;Sox11$^{fl/fl}$;Sox12$^{-/-}$: 129SvEx:C57BL/6	Obtained from the colony of V. Lefebvre (Cleveland Clinic); Bhattaram et al., 2010	N/A
Mouse: WT: C57BL/6	The Jackson Laboratory	Strain: #000664
Recombinant DNA		
RNA probe: Plexin-A1	Yoshida et al., 2006	N/A
RNA probe: Nr-CAM	Williams et al., 2006	N/A

(Continued on next page)

Continued

REAGENT or RESOURCE	SOURCE	IDENTIFIER
RNA probe: EphB1	Williams et al., 2003	N/A
RNA probe: Neuropilin1	Yoshida et al., 2006	N/A
RNA probe: Sox4	Dy et al., 2008	N/A
RNA probe: Sox11	Dy et al., 2008	N/A
RNA probe: Sox12	Dy et al., 2008	N/A
RNA probe: Hes5	Gift of R. Kageyama (University of Kyoto); Akazawa et al., 1992	N/A
RNA probe: Notch1	Reaume et al., 1992	N/A
FLAG-Sox4	Dy et al., 2008	N/A
FLAG-Sox11	Dy et al., 2008	N/A
FLAG-Sox12	Dy et al., 2008	N/A
CMV-Notch intracellular domain (NICD)	Gift of H. Okano, (University of Keio); Matsuda et al., 2012	N/A
CAG-GFP	Petros et al., 2009	N/A
CAG-Cre	Matsuda and Cepko, 2007	Addgene plasmid: #13775
CAG-ER^{T2}CreER^{T2}	Matsuda and Cepko, 2007	Addgene plasmid: #13777
CAG-Hes5	This paper; original Hes5 cDNA from R. Kageyama (University of Kyoto)	N/A
pGL3-Hes5 (−2767 to −2244) reporter plasmid	Gift of H. Okano, (University of Keio); Matsuda et al., 2012	N/A
pGL4.10-Plexna1 (−3085 to −2386) reporter plasmid	This paper	N/A
pGL4.10-Nrcam (−1001 to +15) reporter plasmid	This paper	N/A
pRL-Renilla luciferase plasmid	Promega	Cat#AF025846
Sequence-Based Reagents		
Primer for Chip: Plexina1 Forward: 5′-GTCCACAACCATAAGG CTCCA-3′, Reverse: 5′-GCTCTCTCCCAACTCTGAGTAACA-3′	This paper	N/A
Primer for Chip: Nrcam Forward: 5′-GGTTTCTGAAAAACAA CCAGGA-3′, Reverse: 5′-AAGGTGCCCATCTTCCTGTC-3′	This paper	N/A
Primer for qRT-PCR: Hes5 Forward: 5′-AAGAGCCTGCACC AGGACTA-3′, Reverse: 5′-CGCTGGAAGTGGTAAAGCA-3′	Tiberi et al., 2012	N/A
Primer for qRT-PCR: Hes1 Forward: 5′-TCTGACCACAGAAA GTCATCA-3′, Reverse: 5′-AGCTATCTTTCTTAAGTGCATC-3′	Tiberi et al., 2012	N/A
Primer for qRT-PCR: Ccnd1 Forward: 5′-TGCCATCCATGCG GAAA-3′, Reverse: 5′-AGCGGGAAGAACTCCTCTTC-3′	Kothapalli et al., 2007	N/A
Primer for qRT-PCR: Gapdh Forward 5′-TGACCACAGTCCAT GCCATC-3′:, Reverse: 5′-CATACCAGGAAATGAGCTTGAC-3′	Usui et al., 2013	N/A
Software and Algorithms		
UCSC Genomic Browser	UCSC	https://genome.ucsc.edu/
TESS	Schug, 2008	http://www.cbil.upenn.edu/tess
PROMO	Messeguer et al., 2002	http://alggen.lsi.upc.es/cgi-bin/promo_v3/promo/promoinit.cgi?dirDB=TF_8.3

CONTACT FOR REAGENT AND RESOURCE SHARING

Further information and requests for reagents should be directed to and will be fulfilled by the Lead Contact, Carol Mason (cam4@columbia.edu).

EXPERIMENTAL MODEL AND SUBJECT DETAILS

Animals

All animal experiments were performed according to the regulatory guidelines of the Columbia University Institutional Animal Care and Use Committee. Generation of $Sox4^{flox/flox}$ mutant mice (strain background; 129SvEx:C57BL/6) has previously been described (Penzo-Méndez et al., 2007). Generation of $Sox11^{flox/flox}$, $Sox12^{-/-}$ and $Sox4^{flox/flox}Sox11^{flox/flox}Sox12^{-/-}$ mutants (strain background; 129SvEx:C57BL/6) has previously been described (Bhattaram et al., 2010). The triple mutant mice were obtained from the colony of Véronique Lefebvre, Cleveland Clinic, and maintained at Columbia University. Breeding of $Sox4^{flox/flox}Sox11^{flox/flox}Sox12^{-/-}$ mice produced embryos of the same genotype, which were used in all in vivo and culture experiments. C57BL/6 wild-type embryos were used as a negative control. Single, double, or triple SoxC mutants for the in vitro analysis in Figure 2E were generated by breeding heterozygous $Sox4^{f/+}Sox11^{f/+}Sox12^{-/+}$ mice, which are the offspring of $Sox4^{flox/flox}Sox11^{flox/flox}Sox12^{-/-}$ and C57BL/6 wild-type mice. Genotyping of each embryo was carried out by PCR for $Sox4^{+}$ or $Sox4^{flox}$ allele-specific segments with the primers FP: 5′-GAAGGAGGCGGAGAGTAGACG G- 3′, and RP: 5′ -CATAGCTCAACACAAATGCCAACG C- 3′, for $Sox11^{+}$ or $Sox11^{flox}$ allele-specific segments with the primers FPA: 5′ -TTCGTGATTGCAACAAAGGCGGAG- 3′ and RPA: 5′ -GCTCCC TGCAGTTTAAGAAATCGG- 3′, and for $Sox12^{+}$ allele with the primers FPA: 5′ -CCTTCTTGCGCATGCTTGATGCTT- 3′and RP: 5′ -GGAAATCAAGTTTCCGGCGACCAA- 3′ and for the $Sox12^{-}$ allele with the primers FPB: 5′ -ATGCAAATGCTGAGTTCTCTG CCC- 3′ and RP (Bhattaram et al., 2010; Penzo-Méndez et al., 2007). The latter mice are born at roughly Mendelian ratios, are fertile, and survive to adulthood.

All mice were housed in a pathogen-free barrier facility in static polysulfone microisolator cages, up to 5 mice per cage, on autoclaved ALPHA-dri/Cob Blend bedding, at a temperature of 68 - 79°F and 30 - 70% humidity. Mice were maintained in a 12 hr light/dark cycle with acidified water (pH 2.5 - 3.0) and irradiated pelleted diet provided ad libitum. Noon of the day on which a vaginal plug was found was considered E0.5.

The total number of embryos and retinal cultures analyzed for in vivo and in vitro experiments, respectively, from ≥ 3 independent rounds of electroporation was indicated in each figure legend, and the procedures were described in METHOD DETAILS. Embryos were randomly chosen for ex vivo and in utero electroporation, immunostaining and in situ hybridization in each experiment and condition, and these embryos were assigned to each experimental group.

METHOD DETAILS

In situ hybridization and Immunohistochemistry

In situ hybridization with DIG-labeled probes for Sox4, 11, 12 (gifts of V. Lefebvre) (Dy et al., 2008), Notch1 (Reaume et al., 1992), Hes5 (gift of R. Kageyama, Kyoto University, Japan) (Akazawa et al., 1992), EphB1 (Williams et al., 2003), Plexin-A1, Neuropilin1, Nr-CAM (Williams et al., 2006; Yoshida et al., 2006), was performed on 12 μm brain or retinal sections as described previously (Williams et al., 2003). Fluorescent Sox4 mRNA was detected with HNPP fluorescent detection kit (Sigma). The number of Sox4 mRNA^{+} cells expressing Zic2 was counted in a 200 μm x 200 μm area at the border of the VT region adjacent to the SoxC-expressing zone in 3 cryosections including 6 retinal sections caudal to the section with optic nerve, and the number of cells was averaged for each embryo (n = 1). The analysis was repeated in 3 embryos. Immunolabeling was performed with the following primary antibodies: Rabbit IgG anti-GFP (1:500, Thermo Fisher), chick IgG anti-GFP (1:500, Thermo Fisher), mouse IgG anti-Islet1/2 (1:50) (anti-Islet1/2 antibody, was raised against Islet1 expressed in almost all RGCs, and also recognizes Islet2 expressed in a subset of RGCs and co-expressed with Islet1 (Bhansali et al., 2014; Pan et al., 2008; Tsuchida et al., 1994)) and anti-neurofilament (2H3; 1:5; gifts of S. Morton and T. Jessell, Columbia University) (Dodd et al., 1988), mouse anti-Brn3a (1:500, EMD Millipore), rabbit IgG anti-Ki67 (1:500, EMD Millipore), rabbit anti-Zic2 (1:5000; gift of S. Brown, Columbia University) (Brown et al., 2003), mouse anti-Cre (1:200, Abcam). Cy3 (1:500, Jackson) or AlexFluor488 (1:500, Thermo Fisher) were used as secondary antibodies. Hoechst 33258 (1:1000, Thermo Fisher) was used for nuclear staining. Images were captured by a Zeiss Axioplan 2 microscope with an Axiocam digital camera. 300 μm of thick vibratome sections, as in Figure 6D, were imaged on a Zeiss AxioImager M2 microscope with Apotome, AxioCam MRm camera, Neurolucida software (V11.06, MicroBrightField Systems) after immunostaining with GFP and clearing sections with $Clear^{T2}$ (Kuwajima et al., 2013).

Electroporation

In utero and ex vivo electroporation were performed as previously described (Garcia-Frigola et al., 2007; Matsuda and Cepko, 2007; Petros et al., 2009) with minor modifications. 0.3 - 0.5 μL of DNA solution of *CAG-GFP* (0.5 μg/μl) with *CAG-Cre* or *CAG-ER^{T2}CreER^{T2}* (2.0 μg/μl) (gifts of C. Cepko, Harvard University, Addgene plasmids #13775 and #13777) (Matsuda and Cepko, 2007) and/or *CAG-Hes5* (2.0 μg/μl) (gift of R. Kageyama, Kyoto University, Japan) plus 0.03% Fast Green Dye was injected into the subretinal space for in utero or peripheral dorsotemporal (DT) or ventrotemporal (VT) retina for ex vivo electroporation of E14.5 embryos. The "+" electrode of tweezer-type electrodes (CUY650-P7, Nepa Gene) were positioned on the injected eye, and the "-" electrode on the opposite side of the head for *in utero* electroporation. The "+" electrode was positioned on the ventral and dorsal surface of the head for ex vivo electroporation of DT or VT retina. In both types of electroporation 50 ms square current pulses were delivered at 45 V and 950 ms intervals by an electroporator (CUY21EDIT Square Wave, Nepa Gene).

Retinal cell cultures and analysis

For dissociated retinal cell cultures, after ex vivo electroporation, the lens and vasculature were removed and the intact retinal cup was cultured in DMEM/F12 serum-free medium for 24 hr. The eye cup was then dissociated, plated at a density of 70,000 cells in 35 mm glass-bottomed culture dishes, with a 14 mm microwell (MatTek Corp.) coated with poly-L-ornithine (Sigma) and laminin (Thermo Fisher) in DMEM/F12 serum-free medium containing 0.4% methylcellulose (Sigma). Dissociated retinal cells were fixed for 20 min with 4% PFA. For quantification in dissociated retinal cultures of Islet1/2$^+$ and Ki67$^+$, and in later experiments, of Cre$^+$ or Brn3a$^+$/GFP$^+$ cells (%), for each experiment, 5 electroporated eye cups were pooled, dissociated, and divided into 2 wells for the analysis. For Figure 2E, 2 electroporated eye cups from each embryo with a different genotype were used for the analysis. In all of these cases, the number of GFP$^+$ cells that were also Islet1/2$^+$, Ki67$^+$, Cre$^+$ or Brn3a$^+$ cells was counted in 5 areas (500 μm x 650 μm /each), in the center and at 12, 3, 6, 9 o'clock in each well, and these numbers were summed and averaged (n = 1 experiment). 3-5 independent rounds of such cultures were repeated for each condition.

For retinal explant cultures, after ex vivo electroporation and culture of electroporated retinal eye cup for 24 hr, GFP$^+$ DT or VT retinal explants were cultured on poly-L-ornithine- and laminin-coated microwell dishes with or without dissociated chiasm cells plated a density of 70,000 cells/dish as described previously (Kuwajima et al., 2012; Wang et al., 1996). For quantification of GFP$^+$ neurite outgrowth in explant cultures, the total area covered by neurites of individual explants was quantified by measuring pixel intensity with ImageJ software. Each experiment was carried out three times, and within each experiment, at least five explants, each from a different embryo/retina were treated in each experimental group. Explants with GFP$^+$ neurites extending from only one region, or explants with few or no axons, independent of the condition, were excluded from quantitative analysis. 4OHT (final concentration, 1 μM) (Sigma) or DAPT (final concentration, 10 μM) (Sigma) were added into the both cultures at specific times depending on experimental design.

In vivo analysis

Combinations of DNA plasmids were in utero electroporated into E14.5 retina and embryos were fixed at E18.5. For Figures 6, 7, and S8, 1mg of 4OHT (Sigma) diluted in corn oil (Sigma) was intraperitoneally injected into pregnant mothers carrying E16 embryos after electroporation at E14.5. For quantification of Islet1/2$^+$ or Ki67$^+$/GFP$^+$ cells (%) in 12 μm cryosections, all GFP$^+$ cells were found only in non-VT retina in vivo. The number of GFP$^+$ cells that were Islet1/2$^+$, Ki67$^+$ or Cre$^+$ was counted in 3-5 retinal sections, with the middle section at the level of the optic nerve, the numbers were summed, and then percent of GFP$^+$ that were either Islet1/2$^+$ or Ki67$^+$/GFP$^+$ calculated per embryo (n = 1). For each condition, 3-5 embryos from independent individual rounds of in utero electroporation were analyzed. For quantification of retinal decussation of GFP$^+$ axons at the optic chiasm, the average pixel intensity of GFP$^+$ RGC axons in the ipsilateral and contralateral optic tracts in two adjacent sections just caudal to the optic chiasm as shown in Figure 6E, was measured with ImageJ software. The ipsilateral index was obtained by dividing the intensity of the ipsilateral projection by the sum of the contralateral and ipsilateral pixel intensities per embryo (n = 1). For each condition, 4-6 embryos from independent rounds of in utero electroporation were analyzed. The ipsilateral index obtained in mutants was normalized to that in WT embryos. For quantification of GFP$^+$ RGC axon outgrowth in Figure S7, three 20 μm cryosections just rostral to the chiasm, and the subsequent three sections through the optic chiasm were analyzed. The pixel intensity of GFP$^+$ axons within the optic nerve and at the optic chiasm was measured by ImageJ software and the total pixel intensity from the sections of nerve and of chiasm was calculated. The average pixel intensity in these two locations was divided by the total number of GFP$^+$ cells (electroporated) in the retina to give a GFP$^+$ axon outgrowth index per embryo. For each condition, 3-4 embryos from independent rounds of in utero electroporation were analyzed. Data obtained in mutants was normalized to WT.

Luciferase assay

FLAG-Sox4, *Sox11*, or *Sox12* (Dy et al., 2008) was transfected into HEK293 cells or *CAG-GFP* and *CAG-ER^{T2}CreER^{T2}* were electroporated ex vivo into DT or VT retina along with *Hes5* (−2767 to −2244 bp) (gift of Dr. H. Okano, Keio University) (Matsuda et al., 2012), *Plexna1* (−3085 to −2386 bp) or *Nrcam* (−1001 to +15 bp) luciferase reporter constructs (pGL3-*Hes5*, pGL4.10-*Plexna1*, or pGL4.10-*Nrcam*), a *Renilla* luciferase construct (Promega). For the Hes5 reporter assay, the Notch1 intracellular domain (NICD) was also transfected in HEK293 cells. Firefly luciferase activity was measured 48 hr after transfection in HEK293 cells or 24 or 72 hr in cultured retinal cells dissociated as above using Dual-Luciferase Reporter Assay system (Promega).

ChIP assay

After ex vivo electroporation of 0.5 μL of *FLAG-Sox4*, *Sox11*, or *Sox12* or control vector (2.0 μg/μl) and *CAG-GFP* (0.5 μg/μl) into DT retina, whole retina was cultured for 72 hr. 30 GFP$^+$ retinae were cross-linked in 1% formaldehyde in PBS for 10 min at room temperature and used for ChIP assay for each condition, as previously described (Kurita et al., 2006). FLAG-Sox4, Sox11 or Sox12 protein was immunoprecipitated with mouse IgG anti-FLAG or non-immune IgG as a control. qPCR was performed with the following primers: *Plexna1* promoter (120 bp; Forward: 5′ -GTCCACAACCATAAGGCTCCA- 3′, Reverse: 5′ -GCTCTCTCCCAACTCTGAGTAACA- 3′), *Nrcam* promoter (100 bp; Forward: 5′ -GGTTTCTGAAAAACAACCAGGA- 3′, Reverse: 5′ -AAGGTGCCCATCTTCCTGTC- 3′).

qRT-PCR

After ex vivo electroporation of *CAG-GFP* and *CAG-Cre* plasmids into E14.5 WT or *Sox4$^{f/f}$Sox11$^{f/f}$Sox12$^{-/-}$* DT retina, cells from the GFP$^+$ region of the retina were cultured for 48 hr. For total RNA preparation, cells were lysed and RNA was isolated using

CellPress

RNA isolation kit (Thermo Fisher). RNA (100 ng) was reversed transcribed to cDNA. Quantitative PCR was performed in duplicate using Power SybrGreen Mix (Applied Biosystems) and Realplex 4 Mastercycler PCR System (Eppendorf). Results are presented as linearized Ct values normalized to *Gapdh* gene. The results of qRT-PCR in SoxC mutants were normalized to the mean value of WT for each experiment, and experiments were repeated 4 times. Primers for qPCR were previously described: *Hes5* Forward: 5′-AAGAGCCTGCACCAGGACTA- 3′, Reverse: 5′-CGCTGGAAGTGGTAAAGCA- 3′) (Tiberi et al., 2012), *Hes1* (Forward: 5′-TCTGA CCACAGAAAGTCATCA- 3′, Reverse: 5′-AGCTATCTTTCTTAAGTGCATC- 3′) (Tiberi et al., 2012), *Ccnd1* (Forward: 5′-TGCCA TCCATGCGGAAA- 3′, Reverse: 5′-AGCGGGAAGAACTCCTCTTC- 3′) (Kothapalli et al., 2007) and *Gapdh* (Forward 5′-TGACC ACAGTCCATGCCATC-3′:, Reverse: 5′-CATACCAGGAAATGAGCTTGAC- 3′) (Usui et al., 2013).

QUANTIFICATION AND STATISTICAL ANALYSIS

All data were analyzed and graphs were constructed using ImageJ, Microsoft Excel and GraphPad Prism 6 software. All error bars represent the standard error of the mean (SEM), and statistical analysis was determined using unpaired two-tailed Student's t test or one-way ANOVA, two-way ANOVA or three-way ANOVA followed by the Tukey's post hoc test, as indicated in the figure legends associated with each figure. $*p < 0.05$, $**p < 0.01$, $***p < 0.001$, N.S. Not significant ($p > 0.05$).